HHS Public Access

Author manuscript

Biochim Biophys Acta. Author manuscript; available in PMC 2017 October 01.

Published in final edited form as:

Biochim Biophys Acta. 2016 October ; 1860(10): 1579–1595. doi:10.1016/j.bbalip.2015.12.012.

Altered Myocardial Metabolic Adaptation to Increased Fatty Acid Availability in Cardiomyocyte-Specific CLOCK Mutant Mice

Rodrigo A. Peliciari-Garcia[1,2,3], **Mehak Goel**[1], **Jonathan A. Aristorenas**[1], **Krishna Shah**[1], **Lan He**[4], **Qinglin Yang**[4], **Anath Shalev**[5], **Shannon M. Bailey**[6], **Sumanth D. Prabhu**[1], **John C. Chatham**[6], **Karen L. Gamble**[7], and **Martin E. Young**[1]

[1]Division of Cardiovascular Disease, Department of Medicine, University of Alabama at Birmingham, Birmingham, Alabama, USA.

[2]Institute of Biomedical Sciences-I, Department of Physiology and Biophysics, University of Sao Paulo, Sao Paulo, SP, Brazil.

[3]Department of Biological Sciences, Federal University of Sao Paulo, Diadema, SP, Brazil.

[4]Department of Nutrition Sciences, University of Alabama at Birmingham, Birmingham, Alabama, USA.

[5]Division of Endocrinology, Diabetes and Metabolism, Department of Medicine, University of Alabama at Birmingham, Birmingham, Alabama, USA.

[6]Division of Molecular and Cellular Pathology, Department of Pathology, University of Alabama at Birmingham, Birmingham, Alabama, USA.

[7]Division of Behavioral Neurobiology, Department of Psychiatry, University of Alabama at Birmingham, Birmingham, Alabama, USA.

Abstract

A mismatch between fatty acid availability and utilization leads to cellular/organ dysfunction during cardiometabolic disease states (e.g., obesity, diabetes mellitus). This can precipitate cardiac dysfunction. The heart adapts to increased fatty acid availability at transcriptional, translational, post-translational and metabolic levels, thereby attenuating cardiomyopathy development. We have previously reported that the cardiomyocyte circadian clock regulates transcriptional responsiveness of the heart to acute increases in fatty acid availability (e.g., short-term fasting). The purpose of the present study was to investigate whether the cardiomyocyte circadian clock plays a role in adaptation of the heart to chronic elevations in fatty acid availability. Fatty acid availability was increased in cardiomyocyte-specific CLOCK mutant (CCM) and wild-type (WT) littermate mice

Address for correspondence: Martin E. Young, D.Phil., Division of Cardiovascular Disease, Department of Medicine, University of Alabama at Birmingham, 703 19th St. S., ZRB 308, Birmingham, Alabama, 35294, USA, Tel # 205-934-2328, Fax # 205-975-5104, meyoung@uab.edu.

DISCLOSURES

None declared.

for 9 weeks in time-of-day-independent (streptozotocin (STZ) induced diabetes) and dependent (high fat diet meal feeding) manners. Indices of myocardial metabolic adaptation (e.g., substrate reliance perturbations) to STZ-induced diabetes and high fat meal feeding were found to be dependent on genotype. Various transcriptional and post-translational mechanisms were investigated, revealing that *Cte1* mRNA induction in the heart during STZ-induced diabetes is attenuated in CCM hearts. At the functional level, time-of-day-dependent high fat meal feeding tended to influence cardiac function to a greater extent in WT versus CCM mice. Collectively, these data suggest that CLOCK (a circadian clock component) is important for metabolic adaption of the heart to prolonged elevations in fatty acid availability.

Keywords

Chronobiology; contractile function; diabetes; gene expression; metabolism; nutrition

INTRODUCTION

As with various cardiovascular physiologic parameters (*e.g.*, heart rate, blood pressure), clinically-relevant adverse cardiovascular events exhibit a time-of-day-dependence (*e.g.*, myocardial infarctions, sudden cardiac death) [1–6]. The clinical importance of time-of-day-dependent rhythms is supported further by observations that: 1) non-dipping hypertensives exhibit increased left ventricular hypertrophy and are at increased risk of cardiovascular and renal disease (compared to dipping hypertensive subjects) [7, 8]; 2) heart attacks result in larger infarcts when they occur in the early hours of the morning [9, 10]; and 3) that night shift workers have an increased incidence in CVD (relative to day shift co-workers) [11, 12]. Classically, oscillations in cardiovascular parameters have been attributed to fluctuations in stimuli/stressors that are extrinsic to the cardiovascular system (*e.g.*, neurohumoral factors, sheer stress, posture, etc) [2, 13–15]. More recently, there has been an increased appreciation that cardiovascular systems exhibit intrinsic time-of-day-dependent rhythms in various processes, a trait that is mediated by circadian clocks [16–18]. The negative impact of dyssynchrony between intrinsic (i.e., circadian clock) and extrinsic (e.g., behavioral and neurohumoral factors) influences on cardiovascular function was recently highlighted in studies by Martino et al, wherein mutant hamsters harboring a 22 hour internal circadian clock develop CVD when housed in a 24, but not 22, hour light/dark cycle [19]. In addition, our research group has demonstrated that the cardiomyocyte circadian clock directly influences cardiac gene expression, metabolism, and contractile function, and that disruption of this molecular mechanism results in contractile dysfunction and decreased lifespan [20, 21].

Lipid and fatty acid species are more than just a fuel for the contracting myocardium, playing important structural (e.g., lipid bilayer) and signaling (e.g., diacylglycerol activation of PKCs) roles [22–24]. As such, it is essential that synchronization is maintained between fatty acid availability and utilization. This is made possible in various cells, including cardiomyocytes, through a number of feedforward mechanisms, wherein fatty acids promote their utilization. These include post-translational (*e.g.*, stimulation of AMP-activated protein kinase; AMPK) and transcriptional (*e.g.*, activation of peroxisome proliferator-activated

receptor α PPARα) mechanisms [25–27]. Failure to adequately balance fatty acid availability with fatty acid utilization during, for example, obesity and/or diabetes mellitus, leads to accumulation of fatty acyl derivatives (e.g., di- and tri- acylglycerol) within cardiomyocytes, aberrant signaling, contractile dysfunction, and even cell death (*i.e.*, lipotoxicity) [28–30]. These observations highlight a need to understand the mechanisms involved in synchronizing fatty acid availability with utilization.

We have previously reported that the cardiomyocyte circadian clock influences transcriptional responsiveness of the heart to acute changes in fatty acid availability (e.g., fasting) [31]. However, whether this mechanism impacts adaptation of the heart to prolonged elevations in fatty acids at transcriptional, metabolic or contractile function levels, is currently unknown. In order to interrogate this question, the present study challenged wild-type (WT) and cardiomyocyte-specific CLOCK mutant (CCM) mice with increased fatty acid availability for a 9 week period through two distinct strategies; uncontrolled streptozotocin (STZ) induced diabetes mellitus and high fat feeding. In the latter case, mice were fed high fat meals in a time-of-day-dependent manner. As anticipated, in WT hearts STZ-induced diabetes increased reliance on fatty acid oxidation, induced expression of PPARα target genes, but had no significant effects on contractile function (either *ex vivo* or *in vivo*). In contrast, attenuated responses to STZ were observed in CCM hearts at the levels of *cte1* induction (a PPARα target gene) and perturbations in substrate reliance. Similarly, we observed a differential response of WT versus CCM hearts to high fat meal feeding, which included perturbations in oleate and endogenous substrate reliance, as well as glycogen content. Interestingly, time-of-day-dependent high fat meal feeding tended to influence cardiac function to a greater extent in WT versus CCM mice. Collectively, these data suggest that CLOCK (a circadian clock component) is important for metabolic adaption of the heart to prolonged elevations in fatty acid availability.

MATERIALS AND METHODS

Mice

The present study utilized WT and CCM (MHCα-dnCLOCK$^{+/-}$) mice on the FVB/N background, as described previously [20]. All experimental mice were male, and were housed at the Animal Resource Program at the University of Alabama at Birmingham (UAB), under temperature-, humidity-, and light- controlled conditions. A strict 12-hour light/12-hour dark cycle regime was enforced (lights on at 6AM; Zeitgeber Time [ZT] 0); the light/dark cycle was maintained throughout these studies. As such, physiologic diurnal variations were investigated in mice (as opposed to circadian rhythms). For the STZ-induced diabetes study, mice were housed within regular microisolator cages and had free access to standard rodent chow (Teklad Harlan, catalog number 7917). For the high fat diet meal feeding study, mice were housed within a CLAMS (Comprehensive Laboratory Animal Monitoring System), enabling control of food access in a noninvasive automated fashion. All mice received water *ad libitum*. All animal experiments were approved by the Institutional Animal Care and Use Committee of the University of Alabama at Birmingham.

Experimental design

For the STZ-induced diabetes study, mice were divided into one of four experimental groups at 13 weeks of age: 1) WT Vehicle; 2) WT STZ; 3) CCM Vehicle; and 4) CCM STZ. STZ mice received multiple low dose STZ injections, as previously described [32]. Briefly, 40 mg/Kg/day of STZ was injected (IP) in a volume of 100 μL/10 g for 5 consecutive days (total of 200 mg/Kg). Vehicle mice received the same volume of 0.1 mM citrate buffer, pH 4.5. Nine weeks following STZ or vehicle administration, mice were euthanized at one of six time points over the course of the day (ZT0, ZT4, ZT8, ZT12, ZT16, and ZT20), during which time, blood and tissues were collected.

For the high fat diet meal feeding study, mice were allowed access to either a high fat diet (45% calories from fat, Research Diets, New Brunswick, NJ; catalog number D12451) or a control diet (10% calories from fat, Research Diets, New Brunswick, NJ; catalog number D12450B) in a time-of-day-dependent manner. These same diets, which were matched for protein content, have been utilized previously [33, 34]. The feeding regimes for this study are illustrated in Figure 1. Briefly, mice were divided into one of four experimental groups: 1) WT early high fat (EHF) fed; 2) WT late high fat (LHF) fed; 3) CCM EHF fed; and 4) CCM LHF fed. All mice were allowed access to the control diet between ZT0 (*i.e.*, dark-to-light phase transition) and ZT8 (*i.e.*, 8 hours into the light phase). At ZT8, access to food was prevented for all mice; fasting was maintained for a 4-hour period. At ZT12 (*i.e.*, the light-to-dark phase transition), mice in EHF groups were allowed access to the high fat diet for 4 hours. Conversely, mice in the LHF groups were allowed access to the control diet during this time period. At ZT16 (*i.e.*, 4 hours into the dark phase), access to food was prevented for all mice; fasting was maintained for 4 hours. At ZT20, mice in the EHF groups were allowed access to the control diet for 4 hours. Conversely, mice in the LHF groups were allowed access to the high fat diet during this time period. The purpose of the two 4 hour fasting periods was to facilitate gastric emptying prior to, and encourage food consumption upon, subsequent food access. Feeding regimes were maintained daily (starting at 13 weeks of age), for a 9 week period (terminating at 22 weeks of age), through use of the CLAMS; each cage possesses two distinct feeders that open/close in a computer-controlled fashion. Upon completion of the feeding study, mice were euthanized at one of six time points over the course of the day (ZT0, ZT4, ZT8, ZT12, ZT16, and ZT20), during which time blood and tissues were collected.

Whole body behavioral and metabolic monitoring

Twenty-four hour patterns of physical activity (beam breaks), food intake, and energy expenditure (indirect calorimetry) were measured in mice using a CLAMS (Columbus Instruments Inc., Columbus, OH) during week 7 of both studies, as described previously [35].

Body composition assessment

In vivo body composition (total body fat and lean tissue) of mice was determined using an EchoMRI™ 3-in-1 quantitative magnetic resonance (QMR) machine (Echo Medical Systems, Houston, TX). A system test was performed using a known fat standard prior to the measurements being taken. Mice were weighed and then placed into a clear holding tube

capped with a stopper that restricted vertical movement, but allowed constant airflow. The tube was inserted into the machine and the mouse scanned using the Normal Precision mode.

Echocardiographic analysis

Mouse echocardiography was performed under anesthesia with 1.5% isoflurane in 95% O_2, using a VisualSonics VeVo 770 Imaging System (VisualSonics, Toronto, Canada). The High-Resolution System with a RMV707B scanhead equipped with high-frequency 30 MHz probe and data were analyzed using the VisualSonics software package for cardiovascular assessment. The body temperature was maintained between 37.0 °C ± 0.5 °C and heart rate was sustained between 500 ± 100 beats per minute. Systolic and diastolic functions were assessed in mice 8 weeks following STZ administration, as described previously [36]. With regards to diastolic function, mitral valve inflow pattern determines the E/A ratio. E is obtained due to the passive inflow from left atrium (LA) to left ventricle (LV), and A is active inflow when LA contracts. E>A represents a normal mitral valve inflow pattern, while this pattern reverses during impaired relaxation or decreased LV compliance. Increased LA pressure (for example, during hypertrophy due to non-compliance) results in increased passive LV filling (increased E). This causes pseudo-normalization of the E/A ratio as it is indistinguishable from the normal pattern. During diastolic dysfunction, pseudo-normalization of mitral valve inflow pattern occurs suggesting noncompliant LV and increased LA and LV pressures. Mitral valve inflow pattern is preload dependent which means that as the left atrium pressure changes, the E/A measurement changes. Unlike this, the Tissue Doppler imaging (TDI) E/E' is preload independent. TDI of ventricular myocardium immediately adjacent to the mitral valve, gives 2 major waveforms – E' and A'. E' is the early diastolic myocardial relaxation velocity and A' is the myocardial velocity associated with atrial contraction; see Ho and Solomon for additional information [37].

Humoral factor analysis

Following plasma preparation, blood was placed in EDTA-containing tubes and centrifuged at 3,000g for 10 minutes at 4 degrees. Plasma was stored at −80 degrees prior to assessment of glucose, insulin, and non-esterified fatty acids (NEFA) levels using commercially available kits. Glucose was measured on the Stanbio Sirrus analyzer (Stanbio Laboratory, Boerne, TX) using a glucose oxidase reagent (manufactured by Stanbio Laboratory; catalog number 1071–250). Insulin was measured using a sensitive rat insulin RIA kit (manufactured by EMD Millipore Corporation, Billerica, MA; catalog number SRI-13K). NEFA were measured on the Stanbio Sirrus analyzer (Stanbio Laboratories, Boerne, TX) using reagents from Wako Diagnostics, Mountain View, CA (catalog numbers are 999–34691, 995–34791, 991–34891, and 993–35191).

Working mouse heart perfusions

Myocardial substrate utilization and contractile function were measured *ex vivo* through isolated working mouse heart perfusions, as described previously [33, 34, 38, 39]. All hearts were perfused in the working mode (non-recirculating manner) for 30 minutes with a preload of 12.5mmHg and an afterload of 50 mmHg. Standard Krebs–Henseleit buffer was supplemented with 8 mM glucose, 0.4 mM oleate conjugated to 3% BSA (fraction V, fatty

acid-free; dialyzed), 10 μU/ml insulin (basal/fasting concentration), 0.05 mM L-carnitine, and 0.13 mM glycerol. Metabolic fluxes were assessed through the use of distinct radiolabeled tracers: 1) [U-^{14}C]-glucose (0.12mCi/L from MP Biomedicals; glycolysis, glucose oxidation); and 2) [9,10-^{3}H]-oleate (0.067 mCi/L from Sigma-Aldrich; β-oxidation). Measures of cardiac metabolism (*e.g.*, oxygen consumption) and function (*e.g.*, cardiac power) were determined as described previously [33, 34, 38, 39]. At the end of the perfusion period, hearts were snap-frozen in liquid nitrogen and stored at −80°C prior to analysis. Data are presented as steady state values (*i.e.*, values during the last 10 minutes of the perfusion protocol).

Quantitative RT-PCR

RNA was extracted from hearts using standard procedures [40]. Candidate gene expression analysis was performed by quantitative RT-PCR, using methods described previously [41, 42]. For quantitative RT-PCR, specific Taqman assays were designed for each gene from mouse sequences available in GenBank. All quantitative RT-PCR data were normalized to the housekeeping gene *cyclophilin* (this gene did not differ between experimental groups) and is presented as fold change from the WT Vehicle trough value (STZ-induced diabetes study) or the WT EHF trough value (high fat meal feeding study).

Western blotting

Qualitative analysis of protein expression was performed using standard Western blotting techniques, as described previously [39]. Lysates (10 μg) were separated on a 7.5% bis-acrylamide gel by sodium dodecyl sulfate– polyacrylamide gel electrophoresis, transferred to a PVDF membrane and probed with anti-CTE1 (Abcam; catalogue number 133948), anti-phospho-Thr172-AMPK (Cell Signaling; catalogue number 2531), anti-AMPK (Cell Signaling; catalogue number 2532), anti-phospho-ACC (Cell Signaling; catalogue number 3661), anti-ACC (Cell Signaling; catalogue number 3662), anti-NAMPT (Abcam; catalogue number 45890), and anti-acetyl lysine (Cell Signaling; catalogue number 9441) antibodies. Membranes were incubated with either goat anti-rabbit or anti-mouse horse radish peroxidase-conjugated secondary antibody (Santa Cruz; catalogue numbers sc-2004 and sc-2005, respectively). Bands were visualized with Immunstar Western C detection kit (Biorad) on X-ray film, scanned and quantified using Scion Image version 4.0.3.2, and normalized to Calsequestrin (Abcam; catalogue number AB3516); Calsequestrin levels did not differ between experimental groups.

Myocardial Glycogen and Triglyceride

Myocardial glycogen and triglyceride contents were measured from homogenate extracts using enzymatic-based spectrophotometric methods. Glycogen content was assayed using a modified Walaas protocol [43]. Approximately 20mg of heart tissue was dissolved in 1M potassium hydroxide at 70 degrees. An aliquot was acidified using acetic acid, followed by overnight digestion with amyloglucosidase. After neutralization, glucose content in extracts were determined by following NADPH generation from coupled hexokinase/glucose 6-phosphate dehydrogenase reactions (absorbance at 340nm). Total lipids were extracted from heart using a modified Folch procedure [44]. Approximately 25 mg of heart tissue was placed in 5 mL of a 2:1 solution of chloroform and methanol and homogenized using a

Polytron homogenizer (PT1200E, Kinematica, Bohemia, NY). Samples were agitated for 2 hr at room temperature and tissue was filtered. Liquid phases were separated through addition of 1 mL 0.05% sulfuric acid and the bottom phase was obtained. Prior to triglyceride determination, 4 mL of 1% Triton X-100 in chloroform was added and chloroform was evaporated under nitrogen gas. Lipids were dissolved in deionized water. Triglyceride content was determined in triplicate in a 96 well plate using the L-Type TG M colorimetric assay (Wako Diagnostics, Osaka, Japan). Absorbance at 595 nm was determined using a Multiscan Spectrum Microplate Reader (Thermo Scientific). Standards were utilized for both assays, allowing quantification of glycogen and triglyceride levels.

Statistical analysis

Statistical analyses were performed using two- and three-way ANOVA to investigate main effects of time, genotype, and/or intervention (STZ or diet; indicated in Figure panels), followed by Bonferroni's post hoc analyses for pair-wise comparisons. GraphPad Prism (GraphPad Software Version 6.01, San Diego, CA) and Stata version IC10.0 (Stata Corp., San Antonio, TX) were used in the statistical analyses. In all cases, the null hypothesis of no model effects was rejected at $P<0.05$. It is important to note that pair-wise comparisons are indicated on figures only for the effects of STZ-diabetes or high fat meal feeding within a genotype; in contrast, pair-wise comparisons between genotypes are not indicated in the figures (for the sake of simplicity).

RESULTS

Impact of STZ-induced Diabetes on Whole Body Adaptation in Mice

As anticipated, low dose STZ-administration resulted in uncontrolled diabetes in WT mice, as indicated by a marked decrease in plasma insulin levels, and a reciprocal elevation of plasma glucose levels (Figure 2Ai–ii). A Two-way ANOVA also revealed a main effect of STZ administration on plasma NEFA levels, which were elevated in diabetic mice (Figure 2Aiii). Identical observations were made in CCM mice (data not shown).

Next, body weight, body composition, food intake, and physical activity were investigated in both WT and CCM mice challenged with STZ. STZ-induced diabetes attenuated body weight gain in mice, independent of genotype. Throughout the study, body weight gain was attenuated in STZ animals (Figure 2Bi). At the end of the experimental protocol body fat mass was also lower in STZ-treated mice, relative to vehicle controls, again independent of genotype (Figure 2Bii). STZ-induced diabetes also increased food intake and physical activity in mice (STZ main effect). Somewhat surprisingly, a main effect of genotype was observed for physical activity, with a slight decrease in physical activity in CCM mice (Figure 2Bxiii–iv). It is important to note that indirect calorimetry data (e.g., RER) are not reported for this sub-study, given that results obtained from this method during uncontrolled metabolic states (e.g., diabetes) are difficult to interpret, due in part to changes in protein and ketone body metabolism [45].

Differential Metabolic Adaptation of the Heart to STZ-Induced Diabetes in WT versus CCM Mice

Next we investigated whether CCM hearts exhibit a differential response to STZ-induced diabetes at distinct metabolic levels. Initially a sub-set of hearts were isolated and perfused *ex vivo* in the working mode for assessment of cardiac substrate metabolism at ZT6. STZ-induced diabetes significantly increased reliance of the WT heart for oleate (fatty acid) oxidation, with a concomitant decrease on endogenous substrate reliance (Figure 3Ai). In contrast, this effect of STZ-induced diabetes was attenuated in CCM hearts (Figure 3Ai). STZ diabetes did not significantly influence glucose oxidation (although a main effect of genotype was observed, consistent with previous reports [20]; Figure 3Aii). Myocardial oxygen consumption presented an STZ main effect, while ^{14}C-labeled lactate release exhibited no significant differences between experimental groups (Figure 3Aiii–iv). Differences in endogenous substrate reliance prompted assessment of myocardial glycogen and triglyceride levels in the experimental groups in hearts that were frozen immediately following isolation; two-way ANOVA revealed only a genotype main effect for triglyceride levels, which are lower in CCM hearts, consistent with previous reports (Figure 3Av–vi) [34].

Differential metabolic adaptation of CCM hearts to STZ-induced diabetes prompted investigation of candidate transcriptional and posttranslational mechanisms. These included: 1) fatty acid (PPARα) responsive genes; 2) the AMPK/ACC axis ; and 3) the NAMPT/acetylation axis. Metabolism-relevant, established PPARα-target genes (*Cte1, Cd36, Pdk4, Ucp3, Mcad* and *Mcd*) were initially investigated (Figure 3B). As anticipated, STZ-induced diabetes increased expression of the fatty acid responsive genes *Cte1, Cd36, Pdk4, Ucp3*, and *Mcd* in WT hearts; a significant main effect for STZ was not observed for *Mcad* (Figure 3Bi–vi). *Cte1* expression also exhibited a main effect of genotype, being repressed in CCM hearts (Figure 3Bi). Importantly, *Cte1* exhibited a significant STZ-genotype interaction, indicating a blunted induction of this gene in CCM hearts during STZ-induced diabetes (Figure 3Bi). This transcriptional analysis suggested that of the PPARα-target genes investigated, *Cte1* might contribute towards the differential metabolic adaptation of WT versus CCM hearts to STZ-induced diabetes. However, investigation of CTE1 protein levels (at both ZT6 and ZT18) revealed similar levels of induction in WT and CCM hearts in response to STZ-diabetes (i.e., lack of STZ-genotype interaction; Figure 3Bvii–viii).

The AMPK/ACCβ/malonyl-CoA axis plays a critical role in the regulation of myocardial fatty acid oxidation [46, 47]. We therefore hypothesized that this axis may be differentially affected by STZ-induced diabetes in a genotype-specific manner. In order to test this hypothesis, β-AMPK and β-ACCβ were both investigated in hearts isolated at both ZT6 and ZT18, through immunoblotting. In these analyses, a significant increase of in p-AMPK was observed in the hearts of STZ-diabetic mice, independent of genotype (Figure 3Ci–ii). In contrast, no significant differences in p-ACC were observed between the experimental groups (Figure 3Ciii–iv).

Previous studies in the liver suggest that the cell autonomous circadian clock influences β-oxidation through the NAMPT/NAD^+/SIRT/acetylation axis [48]. Consistent with circadian clock control of Nampt, significant time- and genotype- effects were observed for this gene

(Figure 3Di). However, neither a main effect of STZ nor an STZ-genotype interaction was observed (Figure 3Di). Next we investigated NAMPT protein levels, as well as lysine acetylation, in hearts. Consistent with lower *Nampt* mRNA in CCM hearts, NAMPT protein levels were decreased at both ZT6 and ZT18, independent of STZ-induced diabetes (Figure 3Dii–iii). We have previously reported decreased NAD^+ levels in CCM (versus WT) hearts [39], consistent with decreased NAMPT expression. Given that NAD^+ is an essential co-factor for Sirtuins (a family of deacetylases), we next investigated protein acetylation (only at ZT6). Somewhat surprisingly, acetylation was decreased in CCM hearts (main effect of genotype; Figure 3Div). However, neither a main effect of STZ-induced diabetes nor STZ-genotype interaction were observed for protein acetylation (Figure 3Div).

Nine Weeks of STZ-Induced Diabetes did not Influence Contractile Function of the Heart

The data presented in Figure 3 suggests that metabolic adaptation of the heart to STZ-induced diabetes is dependent on the cardiomyocyte circadian clock. Given the close relationship between myocardial metabolism and contractile function, we next investigated numerous parameters of cardiac contractile function for the four experimental groups, both *ex vivo* and *in vivo*.

At the gravimetric level, two-way ANOVA revealed a main effect of both STZ-induced diabetes and genotype on the bi-ventricular weight to tibia length ratio; this parameter was decreased by STZ-induced diabetes and increased in CCM hearts (Table 1). Decreased heart rate was observed in *ex vivo* perfused CCM hearts, independent of STZ-induced diabetes (Table 1). Echocardiography revealed a main effect of genotype on left ventricular posterior wall thickness (Table 1). All other parameters were unaffected by either STZ-induced diabetes or genotype (Table 1). No STZ-genotype interactions were observed for the parameters measured (Table 1). Collectively, these data suggest that 9 weeks of STZ-induced diabetes was not sufficient to induce overt diastolic or systolic dysfunction in mice, and that the cardiomyocyte circadian clock did not influence responsiveness of the heart to STZ-induced diabetes, at the level of contractile function.

Impact of High Fat Diet Meal Feeding on Whole Body Adaptation in Mice

STZ-induced diabetes challenged the heart with an elevation of fatty acid availability independent of the time of day, which was associated with a differential metabolic adaptation of WT versus CCM hearts. Given that circadian clocks influence responsiveness of cells to extracellular stimuli in a time-of-day-dependent manner, we next decided to challenge the heart with increased fatty acid availability at distinct times of the day, through high fat diet meal feeding. High fat meals were given to mice at the beginning or end of the dark phase, since mice are nocturnal. Initially, 24-hour rhythms in food intake (fat consumption) and whole body substrate reliance (indicated by respiratory exchange ratio (RER)) were measured in WT mice in a non-invasive fashion, through use of the CLAMS. As predicted, EHF feeding resulted in a greater proportion of fat-derived calories being consumed at the beginning of the dark phase (relative to LHF feeding; Figure 4Ai). Conversely, LHF feeding resulted in greater fat consumption at the end of the dark phase (Figure 4Ai). Marked time-of-day-dependent differences in RER were observed between the experimental groups (Figure 4Aii). As anticipated, the 4 hour fasting period during the light

phase resulted in a rapid decline in RER, indicative of increased reliance on fatty acid oxidation (Figure 4Aii). Upon consumption of the control diet at the beginning of the dark phase, LHF fed mice increased RER dramatically, reaching a value of approximately 1 (indicative of reliance on carbohydrate oxidation); RER increased to a lesser extent in EHF fed mice at this time (*i.e.*, combination of both fat and carbohydrate oxidation; Figure 4Aii). Fasting for 4 hours during the dark phase resulted in a decline in RER in all mice (Figure 4Aii). Re-feeding at ZT20 increased RER in both groups, with a slight, but significantly greater effect observed in EHF fed mice (Figure 4Aii). Plasma NEFA levels were next measured in the experimental groups at ZT16 and ZT24 (representing the end of the meal feeding phases). Consistent with feeding and RER patterns, at ZT16 plasma NEFA levels tended to be higher in EHF (versus LHF) fed mice. Conversely, at ZT24 plasma NEFA levels were elevated in LHF (versus EHF) fed mice (Figure 4Aiii). Similar observations were made for these parameters in CCM mice (data not shown).

Weekly body weight gain was similar between EHF and LHF fed mice, independent of genotype (Figure 4Bi). At the end of the experimental protocol, body fat was comparable between the four experimental groups (Figure 4Bii). Consistent with achievement of whole body metabolic homeostasis, no differences were observed between the experimental groups for total caloric intake or physical activity (Figure 4Biii–iv).

Differential Metabolic Adaptation of the Heart to High Fat Diet Meal Feeding in WT versus CCM Mice

Myocardial adaptation to time-of-day-dependent high fat diet meal feeding was next investigated; *ex vivo* working mouse hearts were utilized for assessment of cardiac substrate metabolism. Significant diet-genotype interactions were observed for oleate and endogenous substrate reliance, indicating a differential response of WT versus CCM hearts to time-of-day-dependent high fat feeding (Figure 5Ai). More specifically, EHF feeding (relative to LHF) tended to increase reliance on oleate (fatty acid) oxidation in WT hearts, with a concomitant decreased in endogenous substrate reliance; these metabolic fluctuations were absent in CCM hearts (Figure 5Ai). In contrast, neither reliance on glucose oxidation, nor rates of myocardial oxygen consumption and ^{14}Clabeled lactate release were significantly influenced by diet or genotype (Figure 5Ai–iii). Genotype-dependent differences in endogenous substrate reliance were not readily explained by alterations in energy stores; myocardial glycogen content was significantly increased, while triglyceride content tended to be higher, in WT EHF versus LHF hearts prior to *ex vivo* heart perfusions, regardless of genotype (Figure 5Aiv–v). Interestingly, myocardial glycogen content in CCM mice exhibited a significant differential response to time-of-day-dependent high fat meal feeding, as evidenced by a significant diet-genotype interaction (Figure 5Aiv). Collectively, these data reveal a differential metabolic adaptation of CCM hearts to the meal feeding regimes.

Similar to the STZ-induced diabetes sub-study, we next investigated candidate transcriptional and posttranslational mechanisms that might provide mechanistic insight regarding differential adaptation of CCM hearts to high fat diet meal feeding. Investigation of metabolism-relevant PPARα-target genes revealed main effects of the dietary regime for 2 genes (*Cte1* and *Ucp3*) and main effects of time for 5 genes (*Cte1, Cd36, Pdk4, Ucp3*, and

Mcd) (Figure 5Bi–vi). Although distinct genes exhibited diet-time and genotype-time interactions, none exhibited significant diet-genotype interactions, indicating a lack of differential transcriptional adaptation of WT versus CCM hearts to time-of-day-dependent high fat meal feeding. However, it is noteworthy that all 6 genes investigated exhibited a main effect of genotype; given that all mice received a high fat diet meal, and that ad libitum fed control diet mice exhibit a main effect of genotype for only *Cte1* (Figure 5Bi), these observations suggest a differential response of CCM hearts to high fat diet meal feeding (independent of the time at which the meal is give during the dark phase).

Next, we investigated both the AMPK/ACCβ and the NAMPT/acetylation axis (at ZT6). In the former case, no significant effects of genotype or dietary regime were observed for p-AMPK or p-ACC (Figure 5Ci–ii); the non-significant trend towards increased phosphorylation of AMPK and ACC in WT LHF heart is counterintuitive with respect to lower reliance on fatty acid oxidation observed in this experimental group. Similar to the observations in the STZ-induced diabetes study, a main effect of genotype was found for *Nampt* mRNA, NAMPT protein, and protein acetylation (all decreased in CCM hearts; Figure 5Di–iii). However, no diet-genotype interactions were observed for these parameters (Figure 5Di–iii).

Effects of High Fat Diet Meal Feeding on Contractile Function of the Heart

Next, indices of cardiac function were assessed in the four experimental groups (Table 2). For the high fat meal feeding study, no significant differences in the biventricular weight to tibia length ratio were observed with respect to diet (Table 2). Consistent with the STZ-induced diabetes sub-study, a main effect of genotype was observed for the bi-ventricular weight to tibia length ratio (Table 2). Assessment of various cardiac function parameters during ex vivo perfusions revealed only a main effect of genotype for heart rate, which was reduced in CCM hearts (Table 2). Interestingly, there was a trend for increased rate pressure product in EHF fed WT mice compared to LHF fed WT mice (6654±479 and 5796±455 mmHg, respectively; p=0.08); this trend was not observed in CCM hearts (Table 2). Echocardiography was not performed for the high fat diet meal feeding sub-study. Collectively, these data suggest that EHF (versus LHF) feeding may confer improvement in, or maintenance of, cardiac function in a CLOCK-dependent manner.

DISCUSSION

The purpose of the present study was to investigate whether disruption of the cardiomyocyte circadian clock influences adaptation of the heart to prolonged elevations in fatty acid availability (using two distinct models of elevated fatty acid availability in vivo; STZ-induced diabetes and time-of-day-dependent high fat diet meal feeding). The main finding of the study is that CLOCK (a circadian clock component) is important for metabolic adaptation of the heart to elevated fatty acids. More specifically, perturbations in fatty acid oxidation reliance and endogenous substrate reliance in response to STZ-diabetes and high fat meal feeding were attenuated in CCM hearts. Secondary observations included: 1) induction of *Cte1* at the transcriptional level in response to STZ-diabetes is blunted in CCM hearts; and 2) EHF feeding in WT mice tends to improve cardiac function relative to LHF

feeding, an effect that is absent in CCM hearts. Collectively, these data reveal that distinct levels of cardiac adaptation to chronic elevations in fatty acid availability are attenuated in cardiomyocyte-specific CLOCK mutant mice.

We have previously reported that the rodent heart exhibits increased transcriptional responsiveness to fatty acids during the dark/active phase, relative to the light/inactive phase [49]. Furthermore, induction of fatty acid responsive genes in the heart during a 12-hour fast was attenuated in CCM mice, suggesting that acute transcriptional responsiveness of the heart is dependent on the cardiomyocyte circadian clock [31]. More recently, we have reported a differential myocardial response of a distinct genetic model of cardiomyocyte circadian clock disruption (namely cardiomyocyte-specific BMAL1 knockout mice) to acute (16-hour) fasting at the metabolic flux level [21]. However, whether the cardiomyocyte circadian clock impacts adaptation of the heart to prolonged elevations in fatty acids is not known. The current study therefore sought to address this question. STZ-diabetes increased reliance of WT hearts on fatty acid oxidation, which was associated with decreased reliance on endogenous substrate oxidation (Figure 3A). This metabolic switch was attenuated in CCM hearts (Figure 3A). A similar differential response between WT and CCM hearts to EHF versus LHF feeding was observed for fatty acid and endogenous substrate reliance (Figure 5A), as well as glycogen content, revealing an important role for the transcription factor CLOCK in myocardial metabolic adaptation. Interestingly, we have previously reported that hearts isolated from WT mice fed a high fat diet only during the dark/active period exhibit increased rates of fatty acid oxidation relative to WT mice fed the same diet only during the light/sleep phase [33]. Combined with the observations of the current study, we postulate that the first four hours of the dark/active period is a critical time during which exposure of the heart to dietary fatty acids promotes myocardial fatty acid oxidation, which is dependent on a functional CLOCK protein.

Two important questions arose following the observation that CLOCK impacts myocardial metabolic adaptation to chronic elevations of fatty acid levels, namely: 1) by what mechanisms does this occur; and 2) what are the functional consequences? Regarding the former, several possibilities exist, including modulation of transcriptional and post-translational processes. The circadian clock mechanism is primarily transcriptional in nature, consisting of a network of more than 15 transcriptional modulators (of which CLOCK is one) [50]. Direct regulation of metabolically-relevant genes would therefore have the potential to modulate metabolic processes in a time-of-day-dependent manner. Approximately 13% and 8% of the cardiac transcriptome and proteome (respectively) have been shown to oscillate over the course of the day in mice [51, 52]. Many of these gene and protein expression oscillations are lost following genetic disruption of the cardiomyocyte circadian clock (i.e., CCM and CBK mice) [20, 21, 52]. Furthermore, a significant portion of these genes/proteins are directly involved in metabolism. For these reasons, we initially investigated expression of a multiple candidate genes known to encode for key metabolic modulators. This included interrogation of fatty acid responsive genes and known circadian clock controlled genes. Of these, *Cte1* emerged as a potential mechanistic link. Encoding for cytosolic thioesterase 1 [53], the expression of this PPARα-responsive gene during STZ-diabetes and high fat meal feeding was significantly attenuated in CCM hearts (Figures 3B and 5B). Although revealing an important role for CLOCK in transcriptional adaptation of

the heart to fatty acids, the lack of a differential response of CTE1 protein levels in CCM (versus WT) hearts during STZ-induced diabetes suggests that additional mechanisms likely play important roles in linking the cardiomyocyte circadian clock with myocardial metabolic adaptation.

Several post-translational modifications have emerged as being critical not only for signaling from the circadian clock to cellular processes, but also for normal function of the clock itself. These include phosphorylation, ADP-ribosylation, O-GlcNAcylation, and acetylation [39, 54–56]. The AMPK/ACC axis is an excellent example, wherein AMPK activation leads to phosphorylation and inhibition of ACCβ, thereby decreasing malonyl-CoA levels and increasing rates of β-oxidation. However, our findings (Figures 3C and 5C) are not consistent with a major role for this axis in CLOCK modulation of heart responsiveness to fatty acids. The circadian clock is able to affect several posttranslational modifications through influences on cellular NAD^+ levels over the course of the day, via direct regulation of the NAD^+ salvage pathway component NAMPT [48]. In doing so, protein acetylation exhibits a diurnal oscillation in many metabolically-active peripheral tissues, likely via modulation of sirtuins (deacetylases) [57]. A hypothetical model has been proposed for the liver, wherein chronic circadian clock disruption diminishes NAMPT and NAD^+ levels, resulting in increased protein acetylation and inhibition of fatty acid oxidation (through, for example, acetylation of β-oxidation enzymes, such as acyl-CoA dehydrogenases) [48]. Consistent with our previously published observations that CCM mice exhibit decreased myocardial NAD^+ levels [39], here we report diminished *Nampt* mRNA and NAMPT protein levels (Figures 3D and 5D). However, global protein acetylation was significantly decreased (not increased) in CCM hearts (Figure 3D and 5D). These observations, in addition to reports that increased protein acetylation is associated with augmentation of fatty acid oxidation in the heart [58], suggest that alternative mechanisms may be in operation in the heart relative to the liver. It is important to note that the possibility exists that lysine acetylation of distinct, metabolically-relevant proteins (e.g., *MCAD*) could be increased in CCM hearts.

Chronic periods of imbalanced fatty acid availability and utilization can result in accumulation of fatty acyl species within the heart, perturbations in cellular signaling, and even cardiomyocyte apoptosis; if persistent, this may precipitate contractile dysfunction [29]. We therefore investigated whether the cardiomyocyte circadian clock impacted the contractile function response of the heart to increased fatty acid availability. Somewhat surprisingly, 9 weeks of uncontrolled STZ-induced diabetes did not negatively impact cardiac function in either WT or CCM mice (Table 1). In the high fat diet meal feeding sub-study, we observed that hearts from LHF fed WT mice tend to exhibit lower rate pressure product compared to EHF fed mice; this differential response of contractile function to EHF versus LHF feeding was absent in CCM mice (Table 2). Previous studies have reported that WT mice fed a high fat diet during the active (dark) phase exhibit elevated cardiac function and rates of fatty acid oxidation relative to mice fed the same diet during the sleep (light) phase [33]. It is tempting to speculate that consumption of a high fat meal during the first four hours of the active (dark) phase facilitates preservation/improvement of cardiac function by appropriately balancing fatty acid utilization with availability.

In summary, the present study suggests that CLOCK plays an important role in the metabolic adaptation of the heart to prolonged elevations in fatty acid availability. A number of candidate mechanisms linking the cardiomyocyte circadian clock to metabolic adaptation were investigated, although none were established in a causative manner. The study also reports that the time-of-day at which a high fat meal is consumed tends to impact cardiac function (again in a CLOCK-dependent manner). These findings are consistent with the hypothesis that consumption of calorically dense meals at the beginning of the active period potentially elicits benefit to the heart, relative to consumption of such a meal at the end of active period.

Acknowledgments

This work was supported by the National Heart, Lung, and Blood Institute (HL106199, HL074259, HL123574, HL122975). MRI was performed by the UAB Diabetes Research Center Small Animal Physiology Core (DK11015). Humoral factor analysis was performed by the UAB Metabolism Core Laboratory for the Nutrition Obesity Research Center (P30 DK56336, UL 1RR025777, P60DK079626). Echo was performed by the UAB Diabetes Research Center Small Animal Physiology Core (P30DK079626). R.A.P-G scholarship by FAPESP #2012/02443-4). We would like to thank Maximiliano H. Grenett, Betty M. Pat, William F. Ratcliffe, and Uduak S. Udoh for technical assistance.

REFERENCES

1. Carson PA, O'Connor CM, Miller AB, Anderson S, Belkin R, Neuberg GW, et al. Circadian rhythm and sudden death in heart failure: results from Prospective Randomized Amlodipine Survival Trial. J Am Coll Cardiol. 2000; 36:541–546. [PubMed: 10933370]
2. Degaute JP, van de Borne P, Linkowski P, Van Cauter E. Quantitative analysis of the 24-hour blood pressure and heart rate patterns in young men. Hypertension. 1991; 18:199–210. [PubMed: 1885228]
3. Durgan DJ, Young ME. The cardiomyocyte circadian clock: emerging roles in health and disease. Circ Res. 2010; 106:647–658. [PubMed: 20203314]
4. Muller JE, Tofler GH, Stone PH. Circadian variation and triggers of onset of acute cardiovascular disease. Circulation. 1989; 79:733–743. [PubMed: 2647318]
5. Young ME. The circadian clock within the heart: potential influence on myocardial gene expression, metabolism, and function. Am J Physiol Heart Circ Physiol. 2006; 290:H1–H16. [PubMed: 16373589]
6. Young ME. Anticipating anticipation: pursuing identification of cardiomyocyte circadian clock function. J Appl Physiol. 2009; 107:1339–1347. [PubMed: 19608929]
7. Bianchi S, Bigazzi R, Baldari G, Sgherri G, Campese VM. Diurnal variations of blood pressure and microalbuminuria in essential hypertension. Am J Hypertens. 1994; 7:23–29. [PubMed: 8136107]
8. Palatini P, Penzo M, Racioppa A, Zugno E, Guzzardi G, Anaclerio M, et al. Clinical relevance of nighttime blood pressure and of daytime blood pressure variability. Arch Intern Med. 1992; 152:1855–1860. [PubMed: 1387782]
9. Reiter R, Swingen C, Moore L, Henry TD, Traverse JH. Circadian dependence of infarct size and left ventricular function after ST elevation myocardial infarction. Circ Res. 2012; 110:105–110. [PubMed: 22095727]
10. Suarez-Barrientos A, Lopez-Romero P, Vivas D, Castro-Ferreira F, Nunez-Gil I, Franco E, et al. Circadian variations of infarct size in acute myocardial infarction. Heart. 2011; 97:970–976. [PubMed: 21525526]
11. Knutsson A, Akerstedt T, Jonsson BG, Orth-Gomer K. Increased risk of ischaemic heart disease in shift workers. Lancet. 1986; 2:89–92. [PubMed: 2873389]
12. Knutsson A, Boggild H. Shiftwork and cardiovascular disease: review of disease mechanisms. Rev Environ Health. 2000; 15:359–372. [PubMed: 11199246]

13. Muller J, Tofler G, Stone P. Circadian variation and triggers of onset of acute cardiovascular disease. Circulation. 1989; 79:733–743. [PubMed: 2647318]
14. Richards AM, Nicholls MG, Espiner EA, Ikram H, Cullens M, Hinton D. Diurnal patterns of blood pressure, heart rate and vasoactive hormones in normal man. Clin Exp Hypertens A. 1986; 8:153–166. [PubMed: 3521953]
15. Tofler GH, Muller JE, Stone PH, Forman S, Solomon RE, Knatterud GL, et al. Modifiers of timing and possible triggers of acute myocardial infarction in the Thrombolysis in Myocardial Infarction Phase II (TIMI II) Study Group. J Am Coll Cardiol. 1992; 20:1049–1055. [PubMed: 1401601]
16. Scheer FA, Hu K, Evoniuk H, Kelly EE, Malhotra A, Hilton MF, et al. Impact of the human circadian system, exercise, and their interaction on cardiovascular function. Proc Natl Acad Sci USA. 2010; 107:20541–20546. [PubMed: 21059915]
17. Scheer FA, Michelson AD, Frelinger AL 3rd, Evoniuk H, Kelly EE, McCarthy M, et al. The human endogenous circadian system causes greatest platelet activation during the biological morning independent of behaviors. PloS one. 2011; 6:e24549. [PubMed: 21931750]
18. Durgan DJ, Young ME. The cardiomyocyte circadian clock: emerging roles in health and disease. Circ Res. 2010; 106:647–658. [PubMed: 20203314]
19. Martino TA, Sole MJ. Molecular time: an often overlooked dimension to cardiovascular disease. Circ Res. 2009; 105:1047–1061. [PubMed: 19926881]
20. Bray MS, Shaw CA, Moore MW, Garcia RA, Zanquetta MM, Durgan DJ, et al. Disruption of the circadian clock within the cardiomyocyte influences myocardial contractile function, metabolism, and gene expression. Am J Physiol Heart Circ Physiol. 2008; 294:H1036–H1047. [PubMed: 18156197]
21. Young ME, Brewer RA, Peliciari-Garcia RA, Collins HE, He L, Birky TL, et al. Cardiomyocyte-specific BMAL1 plays critical roles in metabolism, signaling, and maintenance of contractile function of the heart. J Biol Rhythms. 2014; 29:257–276. [PubMed: 25238855]
22. Singer SJ, Nicolson GL. The fluid mosaic model of the structure of cell membranes. Science. 1972; 175:720–731. [PubMed: 4333397]
23. Faergeman NJ, Knudsen J. Role of long-chain fatty acyl-CoA esters in the regulation of metabolism and in cell signalling. Biochem J. 1997; 323(Pt 1):1–12. [PubMed: 9173866]
24. McGarry JD. Banting lecture 2001: dysregulation of fatty acid metabolism in the etiology of type 2 diabetes. Diabetes. 2002; 51:7–18. [PubMed: 11756317]
25. Barger PM, Kelly DP. PPAR signaling in the control of cardiac energy metabolism. Trends Cardiovasc Med. 2000; 10:238–245. [PubMed: 11282301]
26. Young ME, McNulty P, Taegtmeyer H. Adaptation and maladaptation of the heart in diabetes: Part II: potential mechanisms. Circulation. 2002; 105:1861–1870. [PubMed: 11956132]
27. Clark H, Carling D, Saggerson D. Covalent activation of heart AMP-activated protein kinase in response to physiological concentrations of long-chain fatty acids. Eur J Biochem. 2004; 271:2215–2224. [PubMed: 15153111]
28. Unger RH. Lipotoxic diseases. Annu Rev Med. 2002; 53:319–336. [PubMed: 11818477]
29. Sharma S, Adrogue JV, Golfman L, Uray I, Lemm J, Youker K, et al. Intramyocardial lipid accumulation in the failing human heart resembles the lipotoxic rat heart. FASEB J. 2004; 18:1692–1700. [PubMed: 15522914]
30. Harmancey R, Wilson CR, Wright NR, Taegtmeyer H. Western diet changes cardiac acyl-CoA composition in obese rats: a potential role for hepatic lipogenesis. J Lipid Res. 2010; 51:1380–1393. [PubMed: 20093477]
31. Durgan D, Trexler N, Egbejimi O, McElfresh T, Suk H, Petterson L, et al. The circadian clock within the cardiomyocyte is essential for responsiveness of the heart to fatty acids. J Biol Chem. 2006; 281:24254–24269. [PubMed: 16798731]
32. Xu G, Chen J, Jing G, Shalev A. Preventing beta-cell loss and diabetes with calcium channel blockers. Diabetes. 2012; 61:848–856. [PubMed: 22442301]
33. Tsai JY, Villegas-Montoya C, Boland BB, Blasier Z, Egbejimi O, Gonzalez R, et al. Influence of dark phase restricted high fat feeding on myocardial adaptation in mice. J Mol Cell Cardiol. 2013; 55:147–155. [PubMed: 23032157]

34. Tsai JY, Kienesberger PC, Pulinilkunnil T, Sailors MH, Durgan DJ, Villegas-Montoya C, et al. Direct regulation of myocardial triglyceride metabolism by the cardiomyocyte circadian clock. J Biol Chem. 2010; 285:2918–2929. [PubMed: 19940111]
35. Bray MS, Ratcliffe WF, Grenett MH, Brewer RA, Gamble KL, Young ME. Quantitative analysis of light-phase restricted feeding reveals metabolic dyssynchrony in mice. Int J Obes (Lond). 2012
36. Ingle KA, Kain V, Goel M, Prabhu SD, Young ME, Halade GV. Cardiomyocyte specific Bmal1 deletion in mice triggers diastolic dysfunction, extracellular matrix response and impaired resolution of inflammation. Am J Physiol Heart Circ Physiol. 2015 ajpheart 00608 2015.
37. Ho CY, Solomon SD. A clinician's guide to tissue Doppler imaging. Circulation. 2006; 113:e396–e398. [PubMed: 16534017]
38. Bray M, Shaw C, Moore M, Garcia R, Zanquetta M, Durgan D, et al. Disruption of the circadian clock within the cardiomyocyte influences myocardial contractile function; metabolism; and gene expression. Am J Physiol Heart Circ Physiol. 2008; 294:H1036–H1047. [PubMed: 18156197]
39. Durgan DJ, Pat BM, Laczy B, Bradley JA, Tsai JY, Grenett MH, et al. O-GlcNAcylation, novel post-translational modification linking myocardial metabolism and cardiomyocyte circadian clock. J Biol Chem. 2011; 286:44606–44619. [PubMed: 22069332]
40. Chomczynski P, Sacchi N. Single-step method of RNA isolation by acid guanidinium thiocyanate-phenol-chloroform extraction. Anal Biochem. 1987; 162:156–159. [PubMed: 2440339]
41. Gibson UE, Heid CA, Williams PM. A novel method for real time quantitative RT-PCR. Genome Res. 1996; 6:995–1001. [PubMed: 8908519]
42. Heid CA, Stevens J, Livak KJ, Williams PM. Real time quantitative PCR. Genome Res. 1996; 6:986–994. [PubMed: 8908518]
43. Walaas O, Walaas E. Effect of epinephrine on rat diaphragm. J Biol Chem. 1950; 187:769–776. [PubMed: 14803461]
44. Folch J, Lees M, Sloane Stanley GH. A simple method for the isolation and purification of total lipides from animal tissues. J Biol Chem. 1957; 226:497–509. [PubMed: 13428781]
45. Simonson DC, DeFronzo RA. Indirect calorimetry: methodological and interpretative problems. Am J Physiol. 1990; 258:E399–E412. [PubMed: 2180312]
46. Dyck JR, Lopaschuk GD. AMPK alterations in cardiac physiology and pathology: enemy or ally? J Physiol. 2006; 574:95–112. [PubMed: 16690706]
47. Beauloye C, Bertrand L, Horman S, Hue L. AMPK activation, a preventive therapeutic target in the transition from cardiac injury to heart failure. Cardiovasc Res. 2011; 90:224–233. [PubMed: 21285292]
48. Peek CB, Affinati AH, Ramsey KM, Kuo H-Y, Yu W, Sena LA, et al. Circadian Clock NAD+ Cycle Drives Mitochondrial Oxidative Metabolism in Mice. Science. 2013:342.
49. Stavinoha M, RaySpellicy J, Hart-Sailors M, Mersmann H, Bray M, Young M. Diurnal variations in the responsiveness of cardiac and skeletal muscle to fatty acids. Am J Physiol. 2004; 287:E878–E887.
50. Takahashi JS, Hong HK, Ko CH, McDearmon EL. The genetics of mammalian circadian order and disorder: implications for physiology and disease. Nat Rev Genet. 2008; 9:764–775. [PubMed: 18802415]
51. Storch KF, Lipan O, Leykin I, Viswanathan N, Davis FC, Wong WH, et al. Extensive and divergent circadian gene expression in liver and heart. Nature. 2002; 417:78–83. [PubMed: 11967526]
52. Podobed P, Pyle WG, Ackloo S, Alibhai FJ, Tsimakouridze EV, Ratcliffe WF, et al. The day/night proteome in the murine heart. Am J Physiol Regul Integr Comp Physiol. 2014; 307:R121–R137. [PubMed: 24789993]
53. Hunt MC, Yamada J, Maltais LJ, Wright MW, Podesta EJ, Alexson SE. A revised nomenclature for mammalian acyl-CoA thioesterases/hydrolases. J Lipid Res. 2005; 46:2029–2032. [PubMed: 16103133]
54. Hardin PE, Yu W. Circadian transcription: passing the HAT to CLOCK. Cell. 2006; 125:424–426. [PubMed: 16678086]
55. Katada S, Sassone-Corsi P. The histone methyltransferase MLL1 permits the oscillation of circadian gene expression. Nat Struct Mol Biol. 2010; 17:1414–1421. [PubMed: 21113167]

56. Tamaru T, Hirayama J, Isojima Y, Nagai K, Norioka S, Takamatsu K, et al. CK2alpha phosphorylates BMAL1 to regulate the mammalian clock. Nat Struct Mol Biol. 2009; 16:446–448. [PubMed: 19330005]

57. Nakahata Y, Sahar S, Astarita G, Kaluzova M, Sassone-Corsi P. Circadian control of the NAD+ salvage pathway by CLOCK-SIRT1. Science. 2009; 324:654–657. [PubMed: 19286518]

58. Alrob OA, Sankaralingam S, Ma C, Wagg CS, Fillmore N, Jaswal JS, et al. Obesity-induced lysine acetylation increases cardiac fatty acid oxidation and impairs insulin signalling. Cardiovasc Res. 2014; 103:485–497. [PubMed: 24966184]

Highlights

1. CLOCK is important for myocardial metabolic adaption to fatty acids.
2. CLOCK disruption attenuates myocardial transcriptional responsiveness to diabetes.
3. High fat meal at the start of the active phase improves myocardial function.

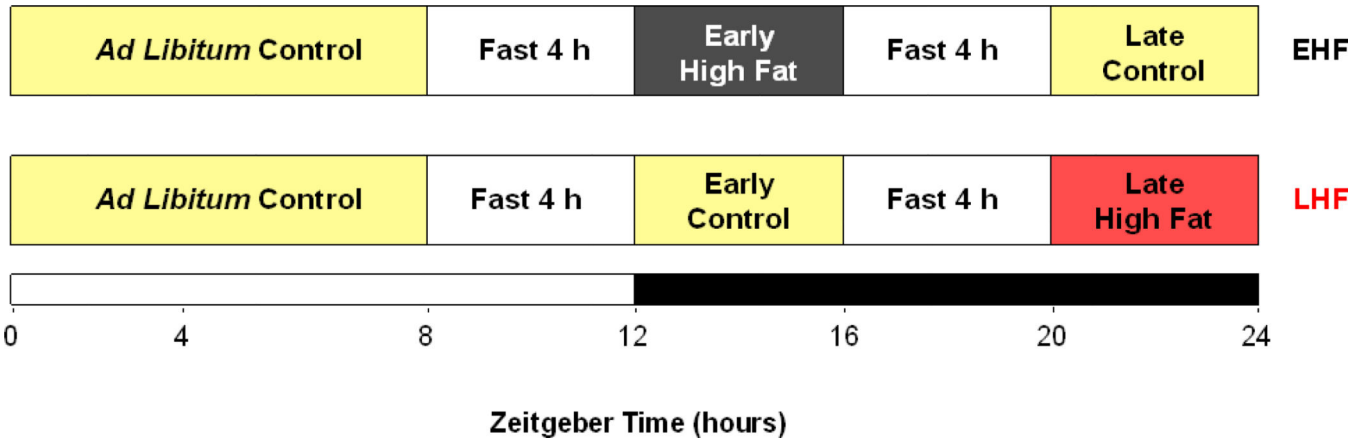

Figure 1.

Experimental design for high fat diet meal feeding study. The diagram illustrates the feeding regimes used in the current study; early (EHF) and late (LHF) high fat diet meal feeding. Mice were fed either control or high fat diets in a time-of-day-dependent manner, as outlined in the figure and in the Methods. Feeding regimes were enforced for a 9 weeks period.

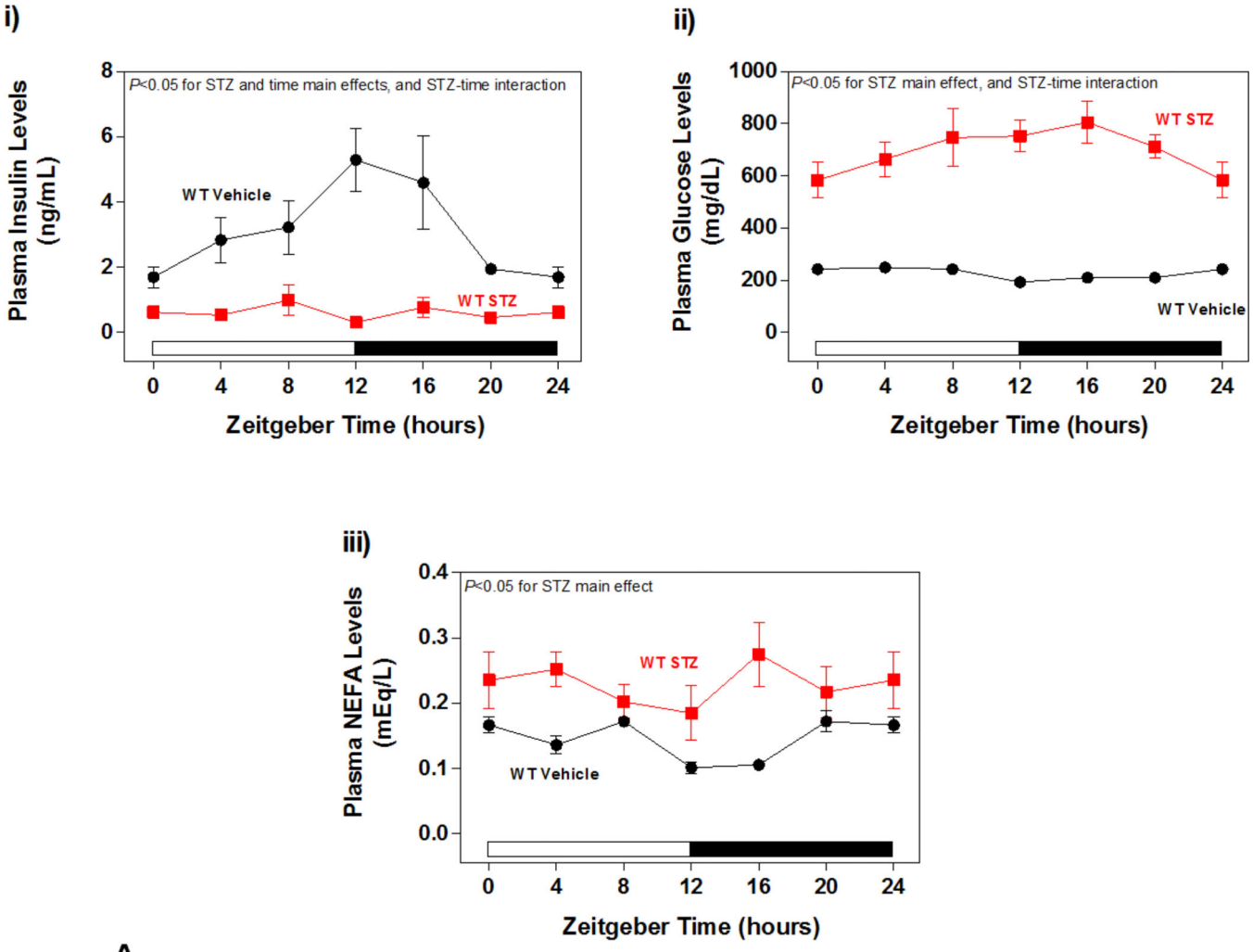

A

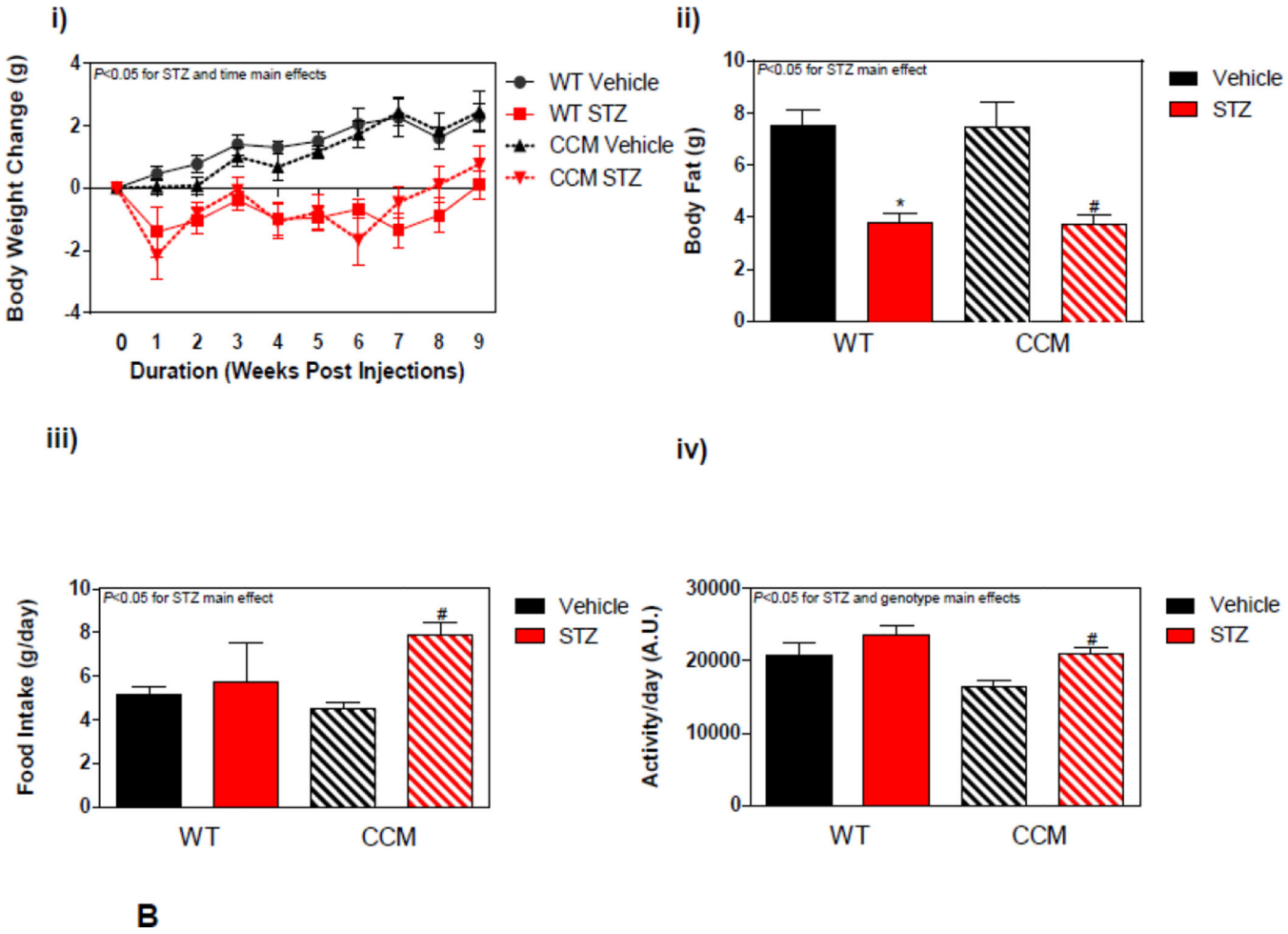

Figure 2.

Impact of STZ-induced diabetes on whole body adaptation in mice. **(A)** i) Plasma insulin, ii) glucose, and iii) NEFA levels in STZ/Vehicle mice. Data shown as mean ± SEM for 6 mice/ZT/experimental group. **(B)** i) Body weight change. ii) body fat, iii) total caloric intake, and iv) physical activity (arbitrary units; A.U.). Data shown as mean ± SEM for 12 mice/experimental group in panel i, and 6 mice/experimental group in panels ii-iii. *, $p<0.05$ for WT vehicle versus WT STZ; #, $p<0.05$ for CCM vehicle versus CCM STZ.

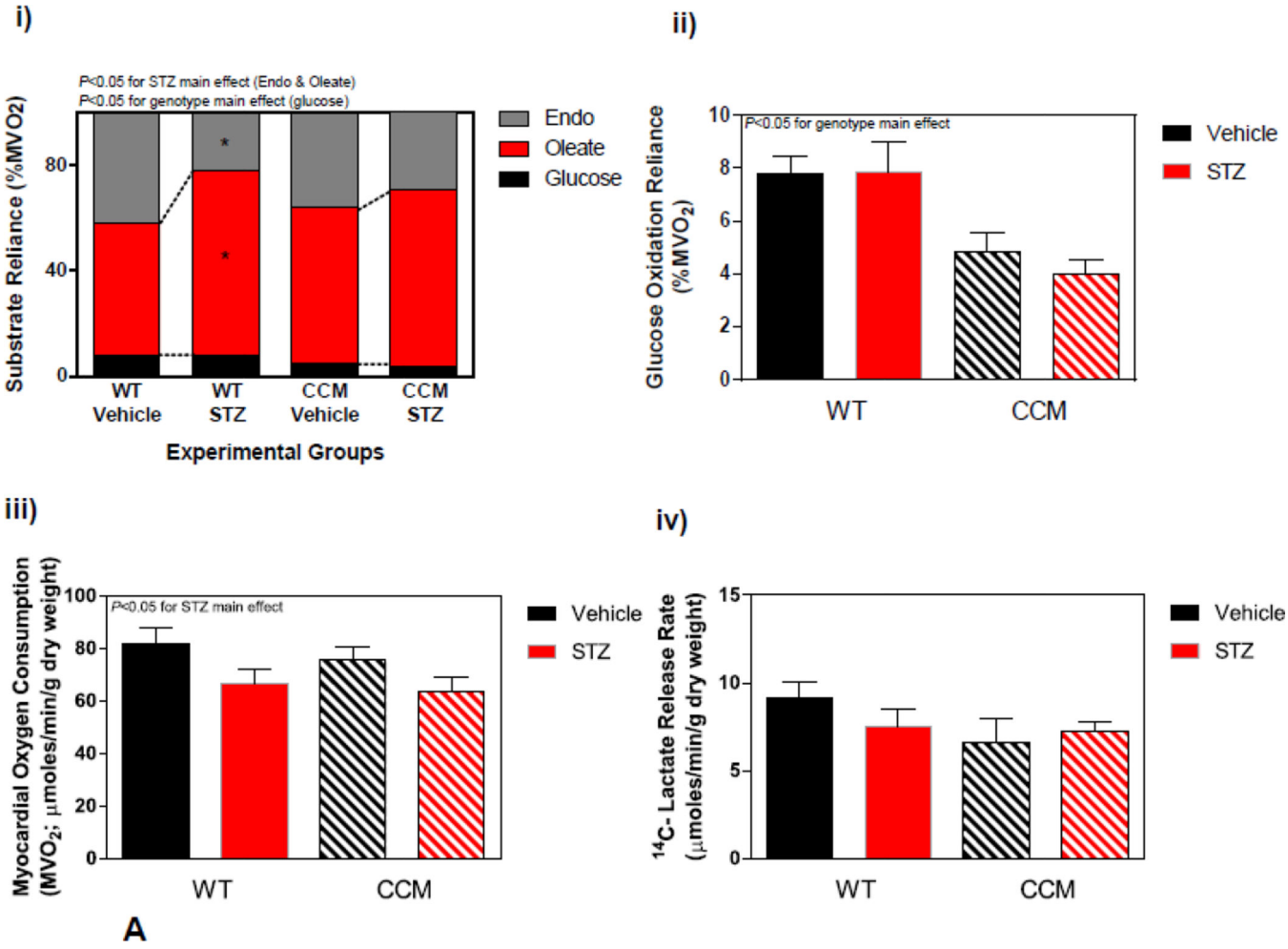

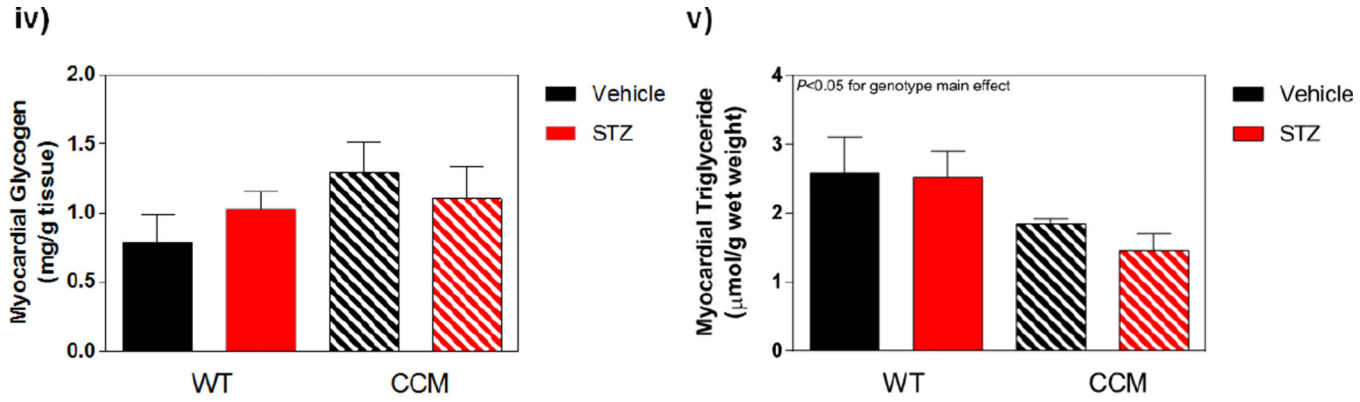

A

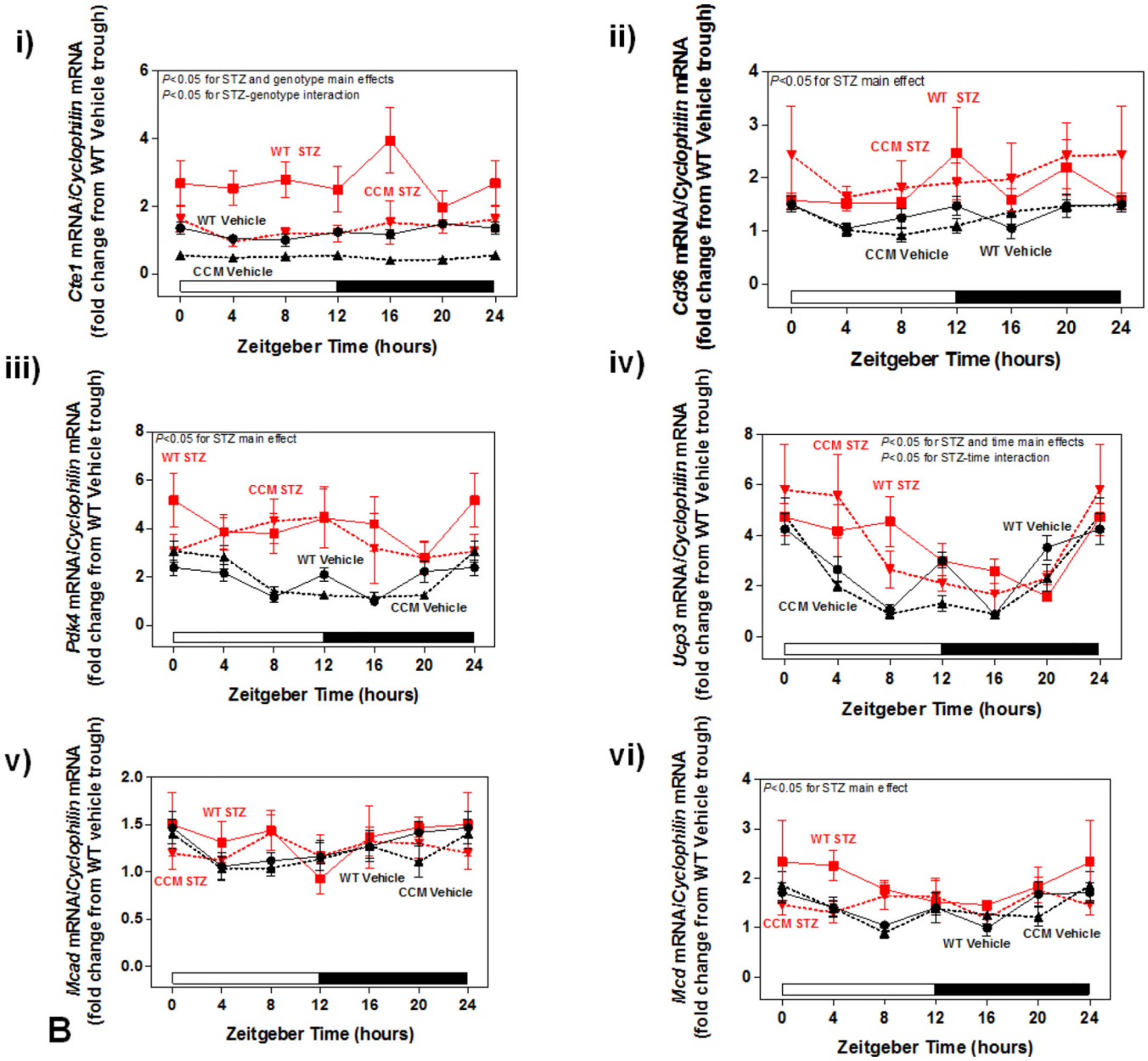

vii)

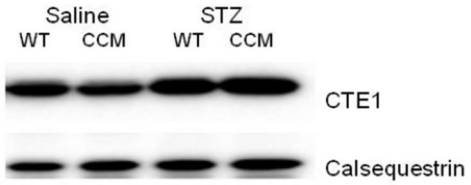

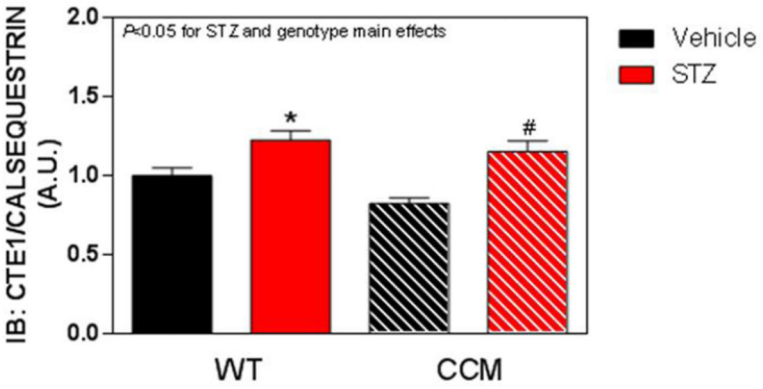

viii)

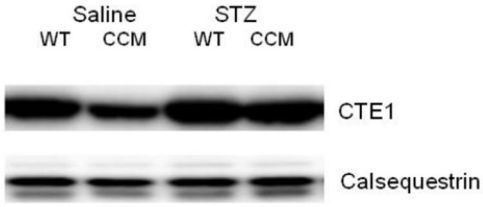

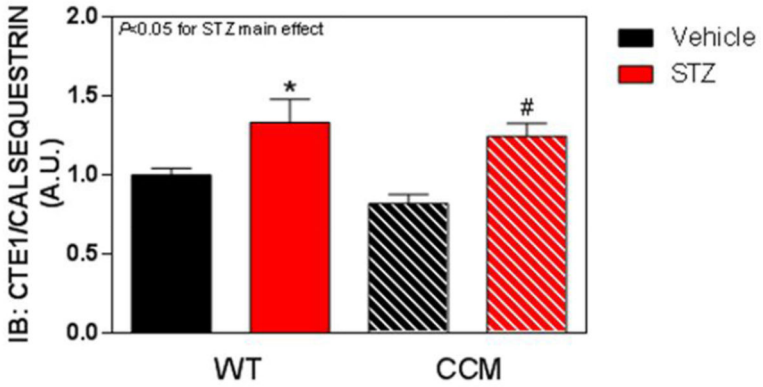

B

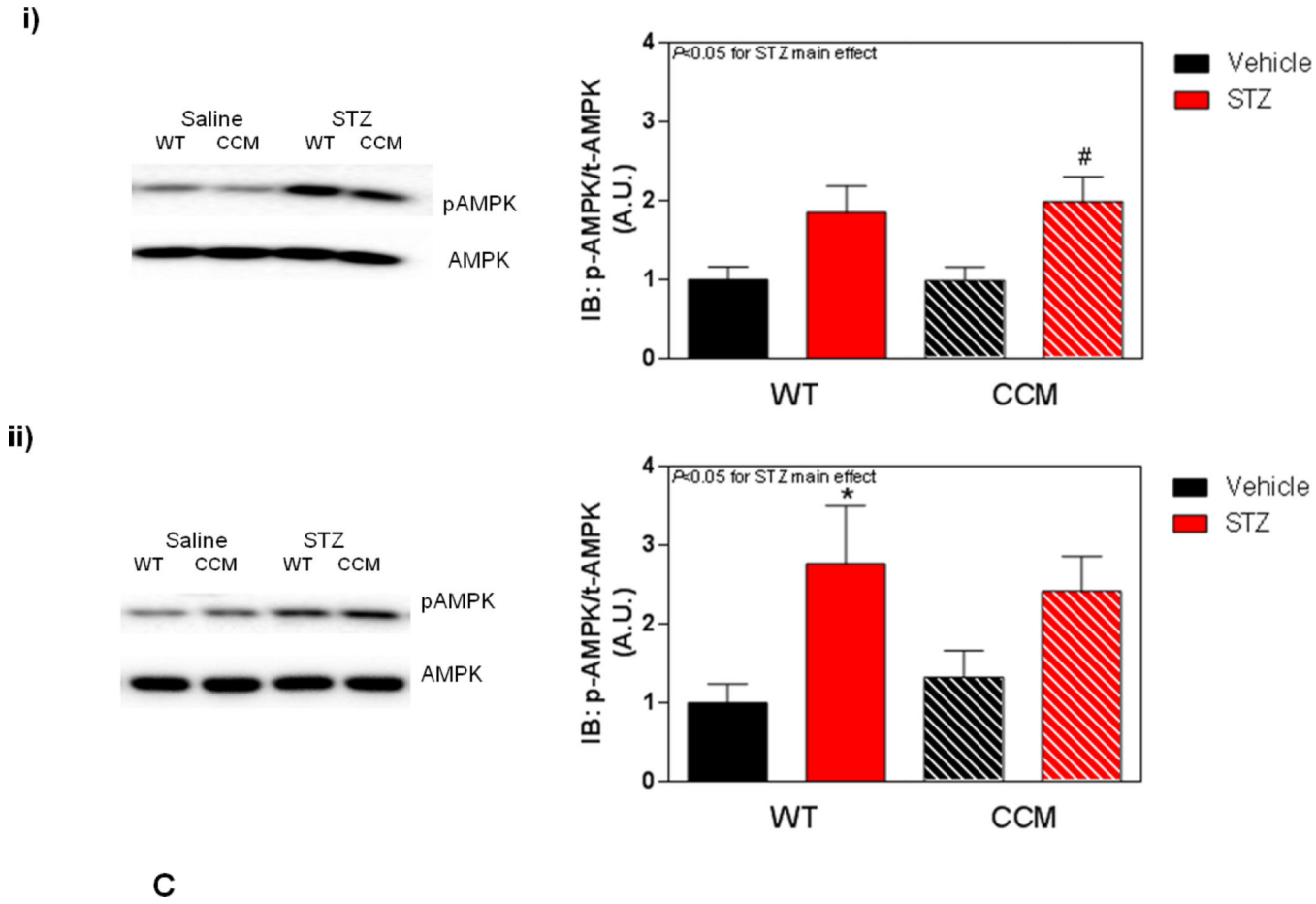

iii)

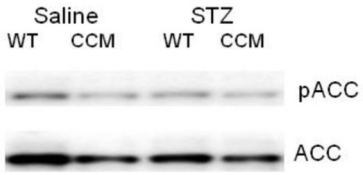

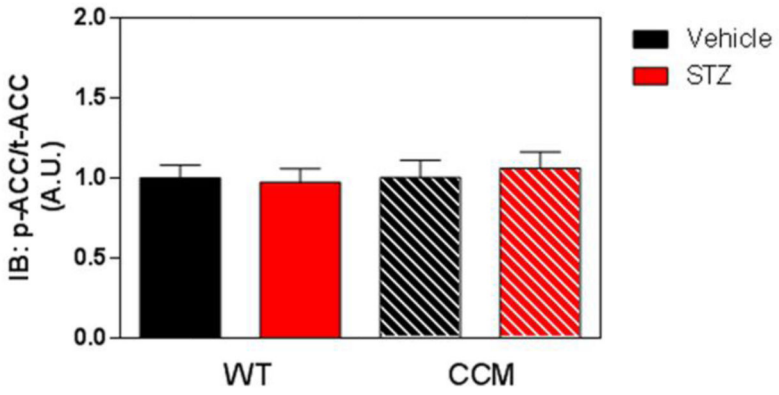

iv)

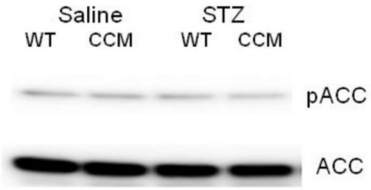

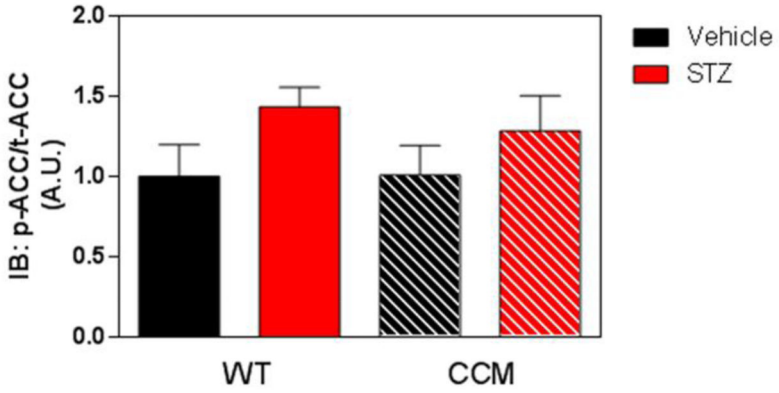

C

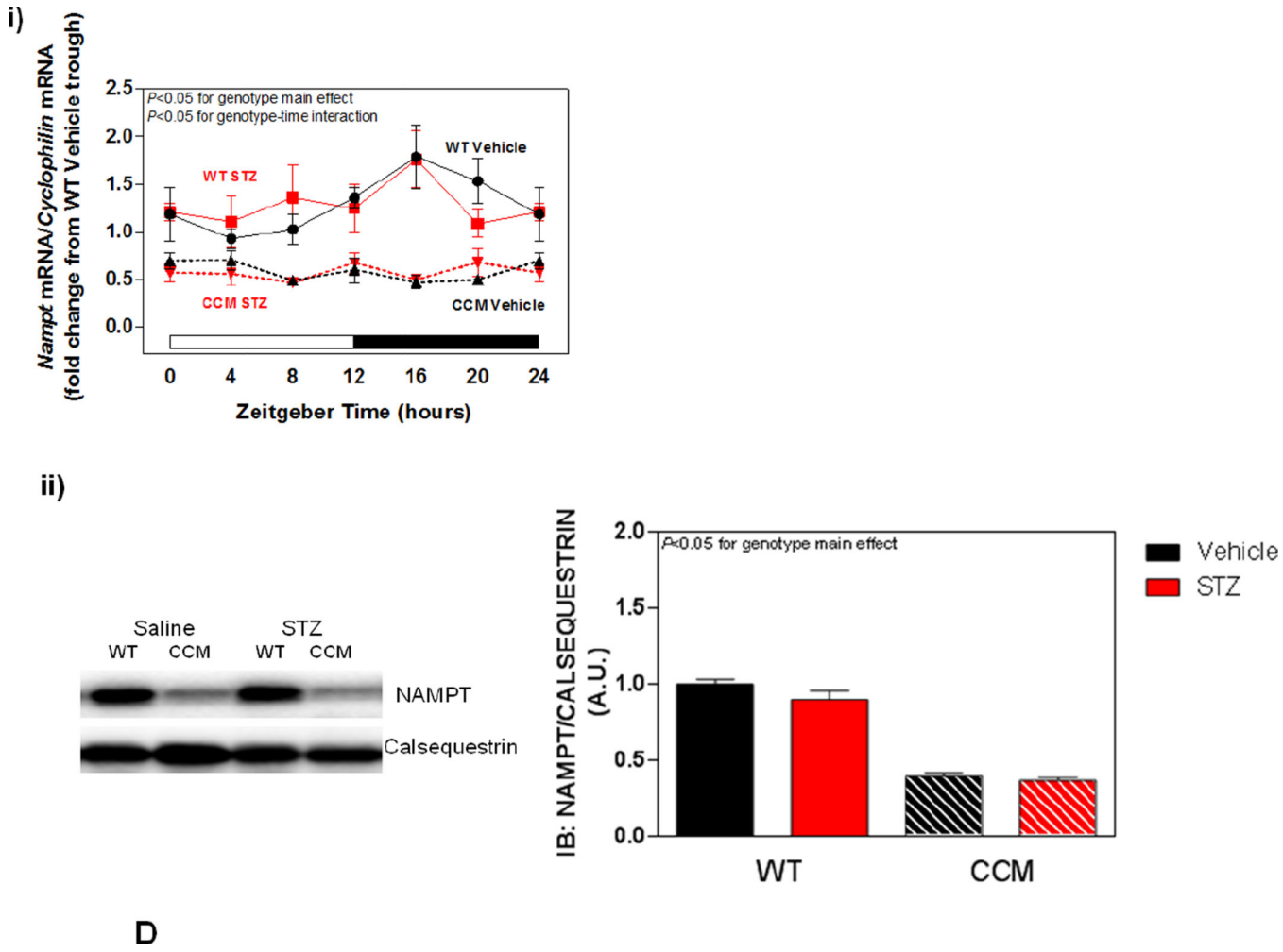

D

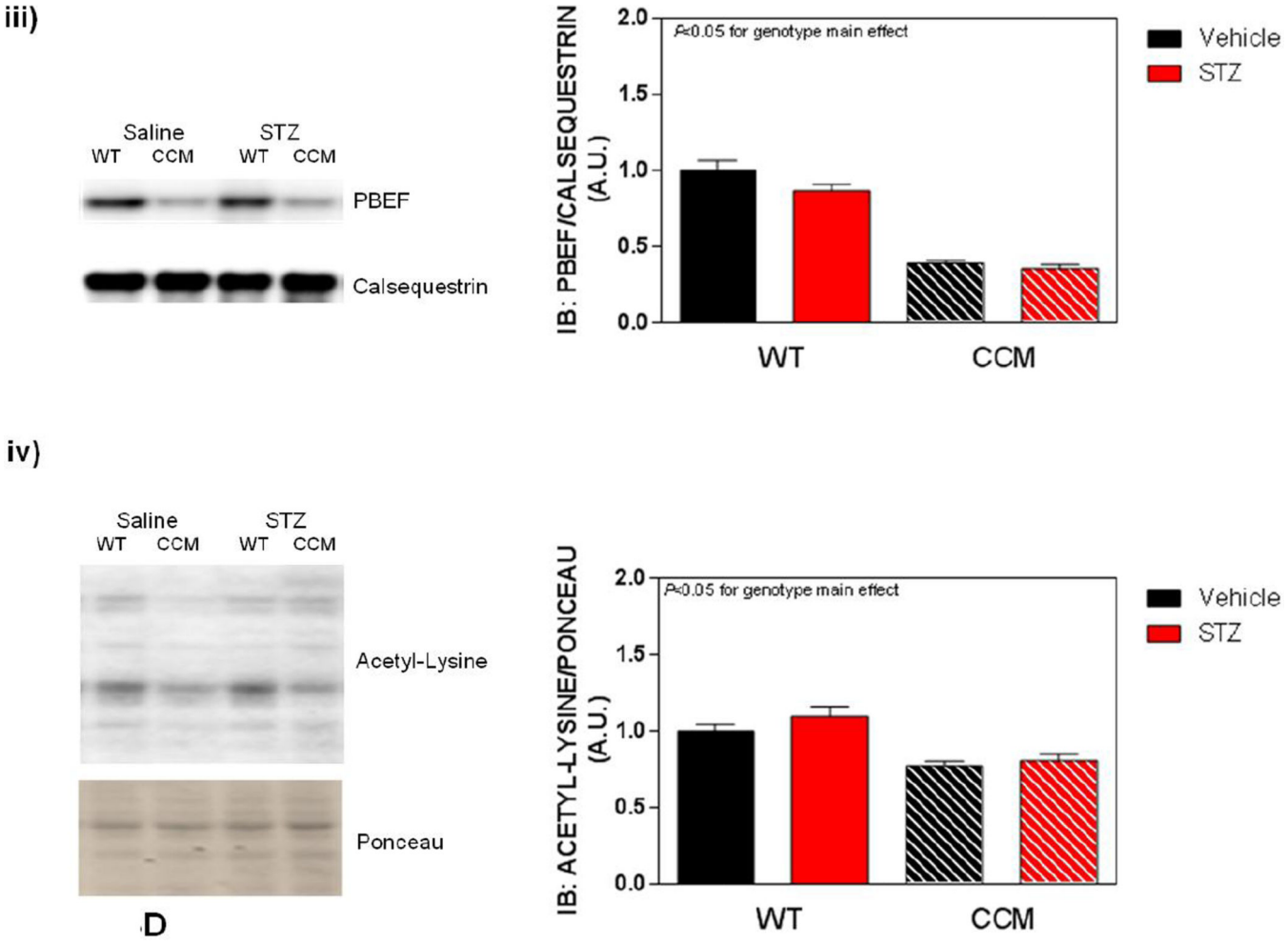

Figure 3.

Differential metabolic adaptation of the heart to STZ-induced diabetes in WT versus CCM mice. **(A)** i) Substrate reliance, ii) Glucose oxidation reliance, iii) myocardial oxygen consumption, iv) ^{14}C-lactate release rate, v) myocardial glycogen levels, and vi) myocardial triglyceride levels. Data shown as mean ± SEM for 6 mice/experimental group. *, $p<0.05$ for WT vehicle versus WT STZ. **(B)** i) *Cte1* mRNA, ii) *Cd36* mRNA, iii) *Pdk4* mRNA, iv) *Ucp3* mRNA, v) *Mcad* mRNA, vi) *Mcd* mRNA, vii) CTE1 protein levels at ZT6, and viii CTE1 protein levels at ZT18. Data shown as mean ± SEM for 6 mice/ZT/experimental group. *, $p<0.05$ for WT vehicle versus WT STZ; #, $p<0.05$ for CCM vehicle versus CCM STZ. **(C)** i) p-AMPK/t-AMPK at ZT6, ii) p-AMPK/t-AMPK at ZT18, iii) p-ACC/t-ACC at ZT6, and iv) p-ACC/t-ACC at ZT6. Data shown as mean ± SEM for 6 mice/experimental group. **(D)** i) *Nampt* mRNA, ii) NAMPT protein levels at ZT6, iii) NAMPT protein levels at ZT18, and iv) protein acetyl-lysine levels at ZT6. Data shown as mean ± SEM for 6 mice/ZT/experimental group.

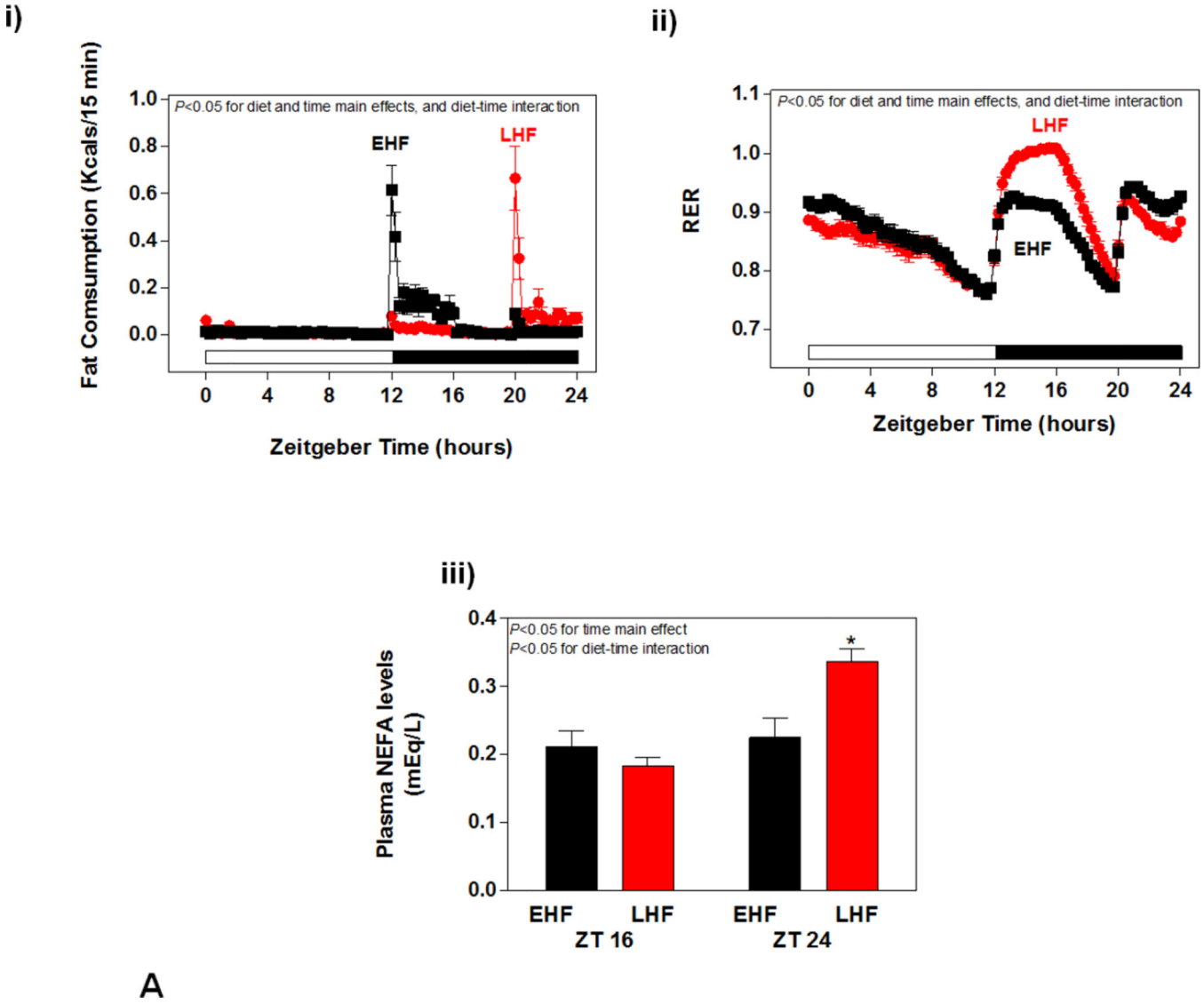

A

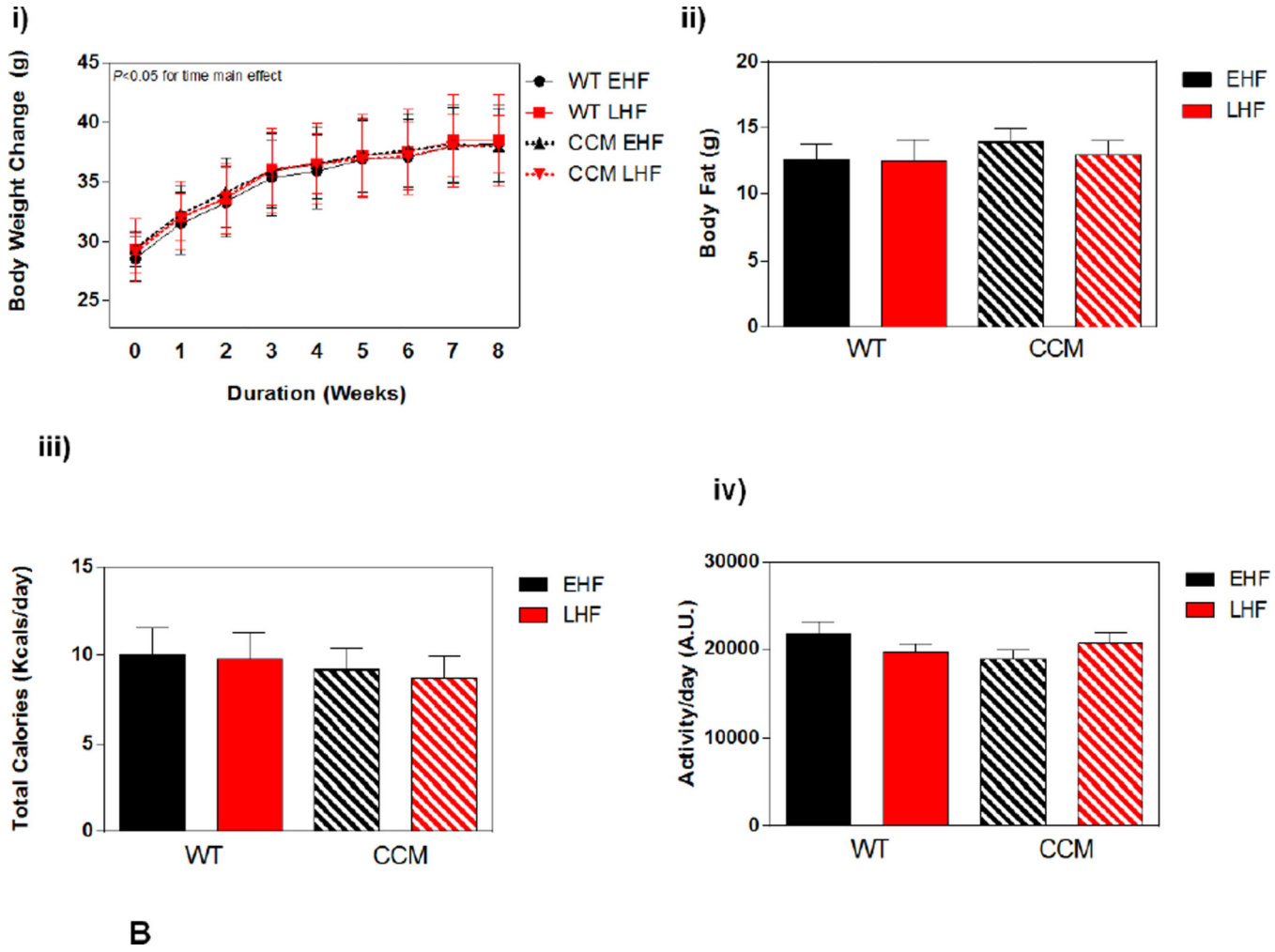

Figure 4.

Impact of high fat diet meal feeding on whole body adaptation in mice. **(A)** i) Fat caloric intake, ii) respiratory exchange ratio (RER), and iii) plasma NEFA levels. Data shown as mean ± SEM for 21 mice/experimental group in panels i-ii and 3 mice/ZT/experimental group in panel iii. *, p<0.05 for EHF vehicle LHF at ZT24. **(B)** i) Body weight change. ii) body fat, iii) total caloric intake, and iv) physical activity. Data shown as mean ± SEM for 6 mice/experimental group in panel ii and 21 mice/experimental group in panels iii-iv.

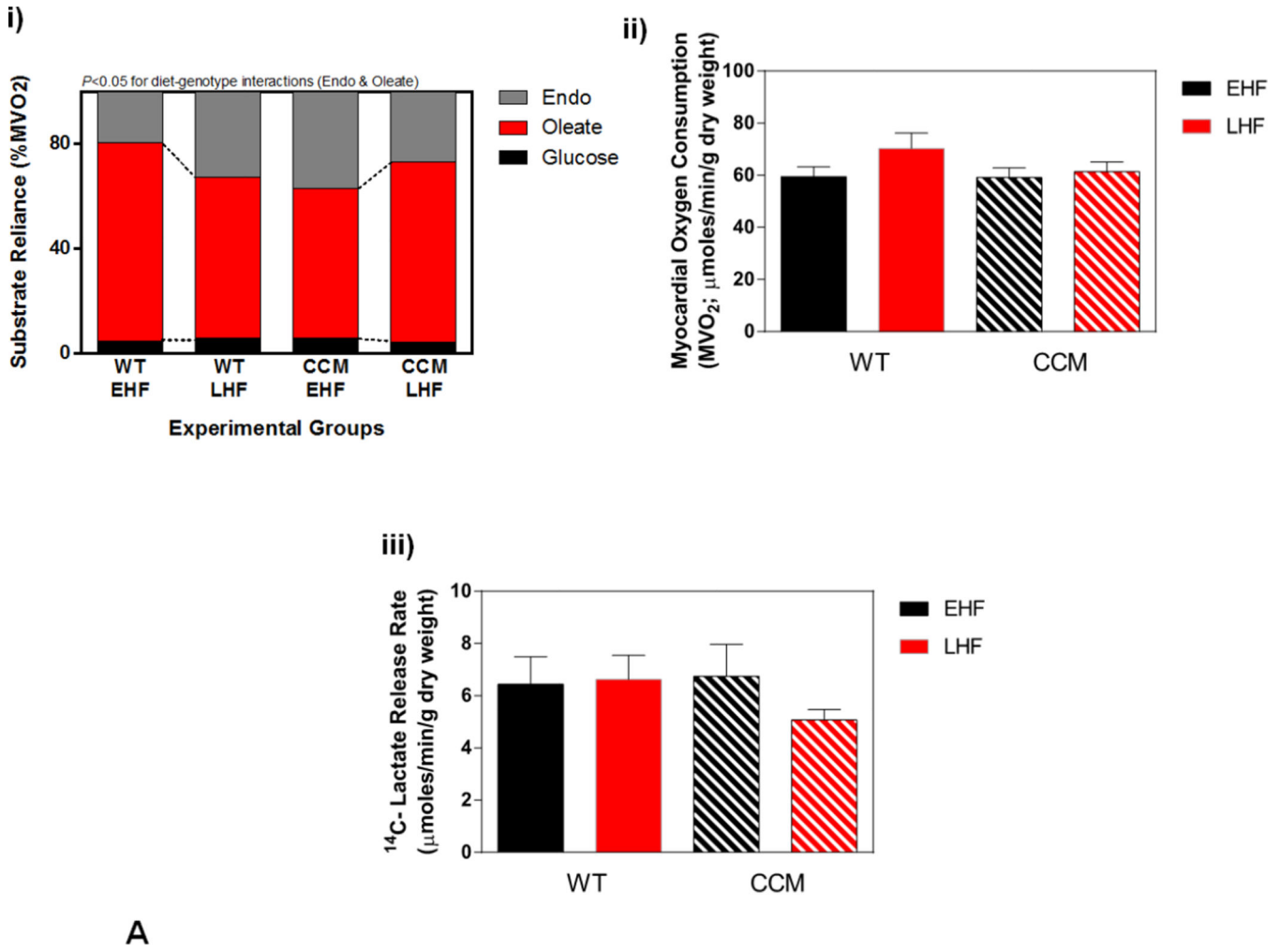

A

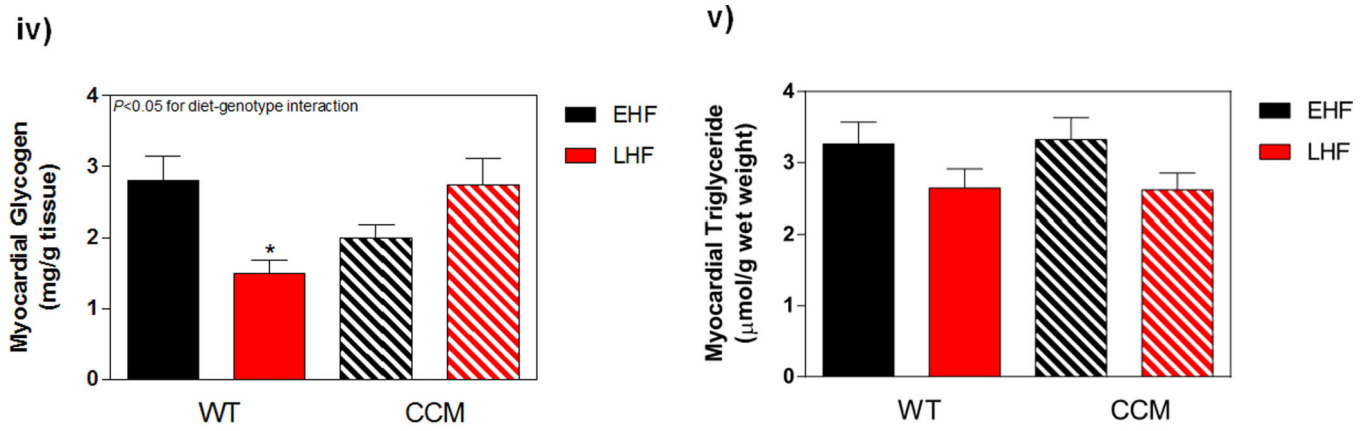

A

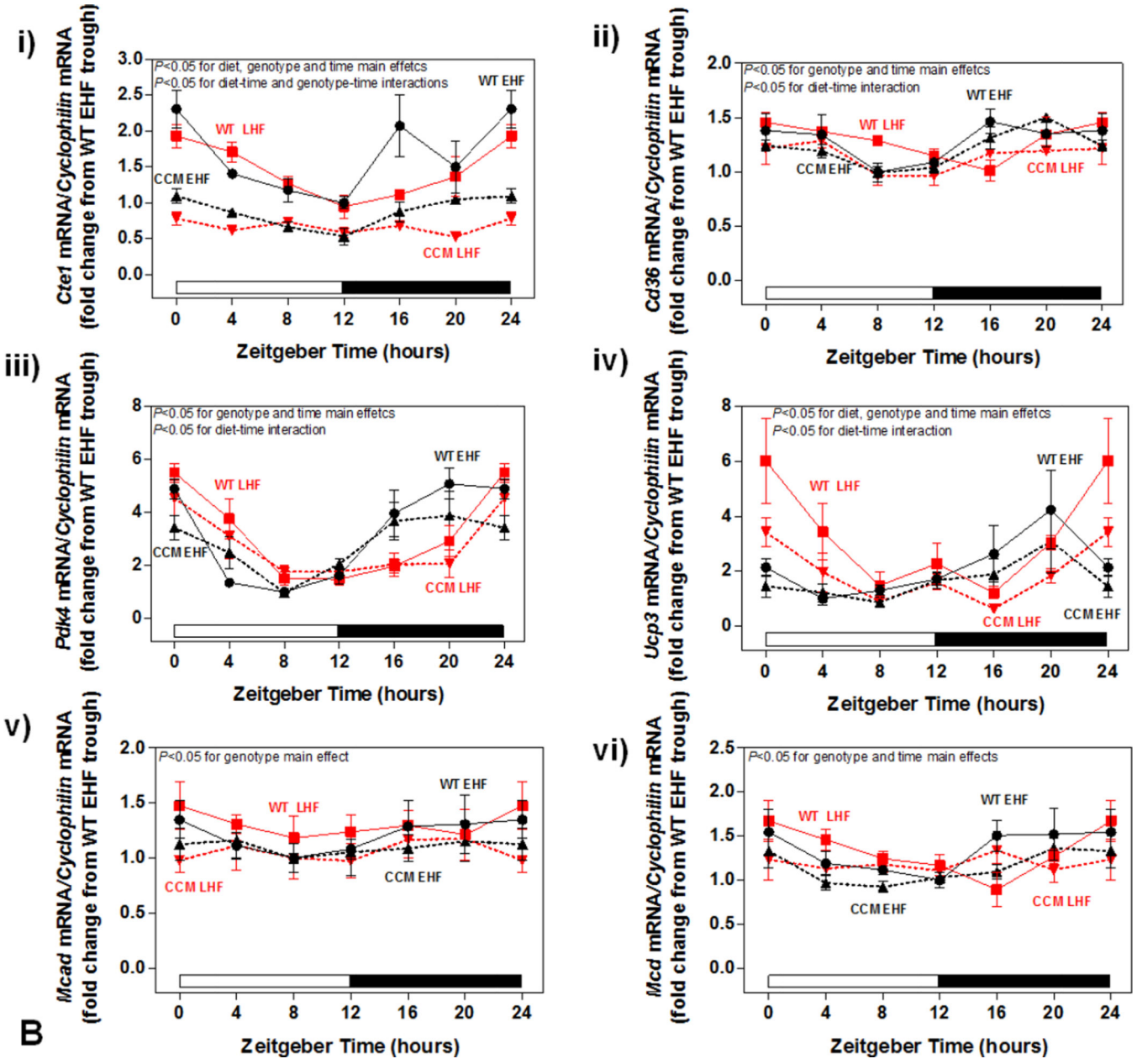

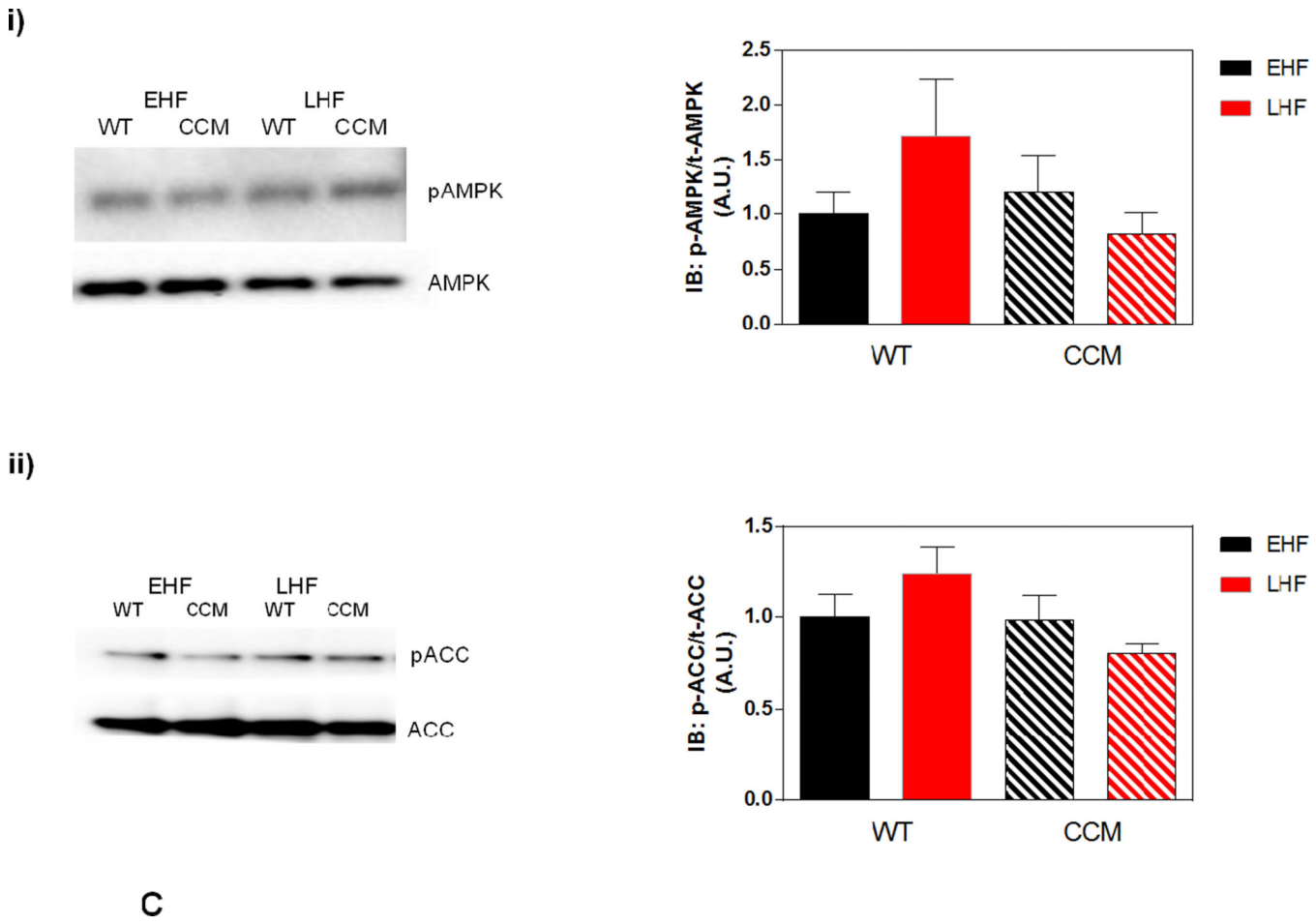

C

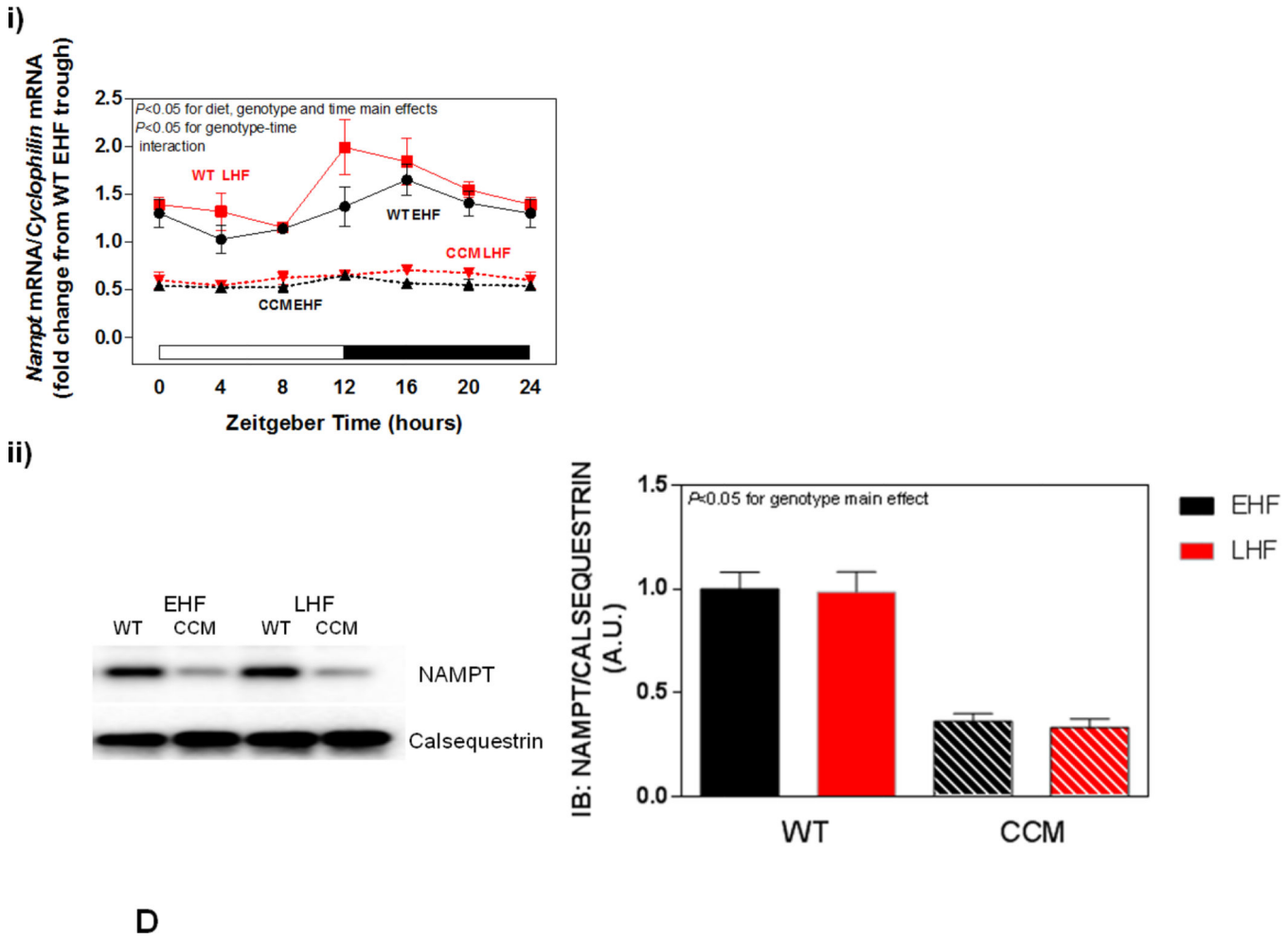

D

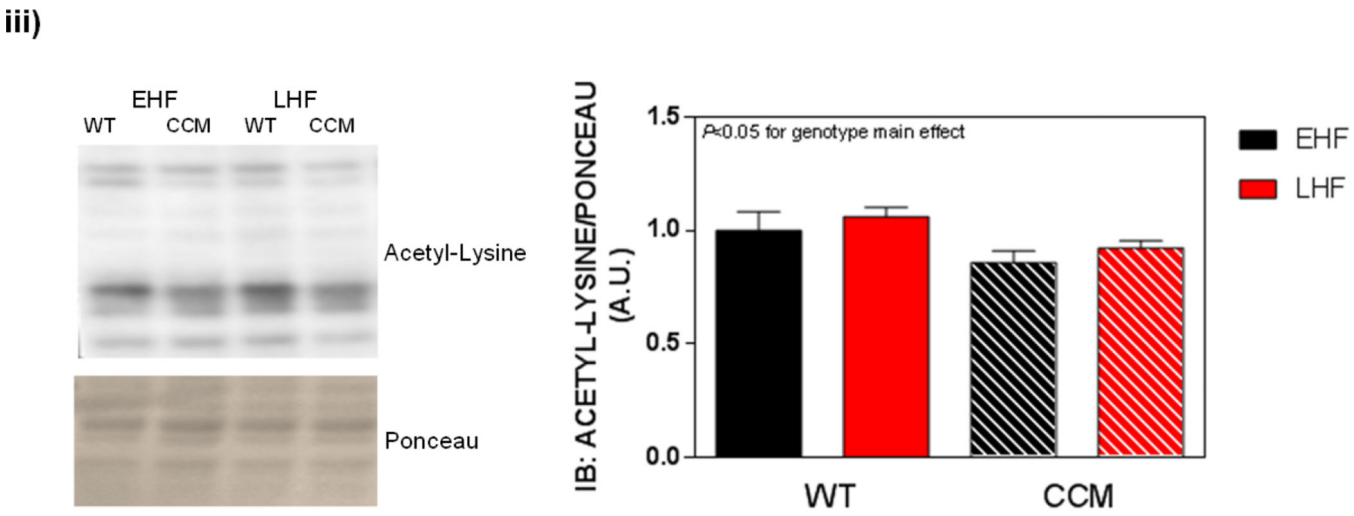

D

Figure 5.

Differential metabolic adaptation of the heart to high fat diet meal feeding in WT versus CCM mice. **(A)** i) Substrate reliance. ii) myocardial oxygen consumption, iii) ^{14}C-lactate release rate, iv) myocardial glycogen levels, and v) myocardial triglyceride levels. Data shown as mean ± SEM for 6 mice/experimental group in panels i-iii and 12 mice/experimental group in panels iv-v. **(B)** i) *Cte1* mRNA, ii) *Cd36* mRNA, iii) *Pdk4* mRNA, iv) *Ucp3* mRNA, v) *Mcad* mRNA, and vi) *Mcd* mRNA. Data shown as mean ± SEM for 6 mice/ZT/experimental group. **(C)** i) p-AMPK/t-AMPK at ZT6, and ii) p-ACC/t-ACC at ZT6. Data shown as mean ± SEM for 6 mice/experimental group. **(D)** i) *Nampt* mRNA, ii) NAMPT protein at ZT6, and iii) protein acetyl-lysine levels at ZT6. Data shown as mean ± SEM for 6 mice/ZT/experimental group.

Table 1

Parameters of cardiac contractile function in the STZ-induced diabetes sub-study.

Analyzed parameters	**WT**		**CCM**	
Ex vivo	**Vehicle**	**STZ**	**Vehicle**	**STZ**
Heart weight (mg)/tibia length (mm)	7.11±0.11	6.90±0.10[a]	8.03±0.11[b]	7.70±0.11[a,b]
Heart rate (bpm)	352±18	347±27	290±28[b]	279±11[b]
Developed pressure (mmHg)	16.5±1.1	19.8±2.2	20.2±1.6	22.2±1.1
Rate pressure product (mmHg*bpm)	5796±455	6654±479	5706±381	6162±242
Cardiac power (mW)	1.15±0.04	1.16±0.08	1.01 ±0.08	1.07±0.07
In vivo				
E/A	1.72±0.06	1.70±0.09	1.62±0.03	1.62±0.07
E/E’	38.0±2.7	31.8±1.3	34.5±2.4	34.8±2.6
Left ventricular fractional shortening (%)	28.2±1.6	30.5±2.1	32.1 ±2.4	30.4±1.8
Left ventricular ejection fraction (%)	54.8±2.5	58.3±2.9	60.2±3.4	57.9±2.6
Left ventricular volume (diastole; μL)	64.6±1.4	57.9±2.7	62.2±2.7	62.8±2.3
Left ventricular posterior wall thickness (diastole; mm)	0.88±0.05	0.91 ±0.02	1.04±0.06[b]	0.93±0.03[b]

Two-way ANOVA:

[a] $p<0.05$ for STZ main effect;

[b] $p<0.05$ for genotype main effect.

Data shown as mean ± SEM for 33 mice/experimental group for heart weight, 6 mice/experimental group for all other ex vivo parameters (working heart perfusions), and 9 mice/experimental group for all in vivo parameters (echocardiography). Mitral valve inflow pattern determines the E/A ratio, where E is obtained due to the passive inflow from left atrium (LA) to left ventricle (LV), and A is active inflow when LA contracts. Tissue Doppler imaging (TDI) E/E’ is preload independent. For additional details, see the Materials and Methods section.

Table 2

Parameters of cardiac contractile function in the high fat diet meal feeding sub-study.

Analyzed Parameters	**WT**		**CCM**	
Ex vivo	**EHF**	**LHF**	**EHF**	**LHF**
Heart weight (mg)/tibia length (mm)	6.84±0.15	6.69±0.10	7.38±0.10^{b}	7.53±0.12^{b}
Heart rate (bpm)	342±19	309±24	278±14^{b}	282±19^{b}
Developed pressure (mmHg)	20.1±1.5	17.5±0.8	19.1±1.6	17.9±2.5
Rate pressure product (mmHg*bpm)	6784±345	5332±317	5277±388	5052±712
Cardiac power (mW)	1.28±0.06	1.27±0.09	1.13±0.09	1.16±0.12

Two-way ANOVA:

^{b}p<0.05 for genotype main effect.

Data shown as mean ± SEM for 21 mice/experimental group for heart weight, and 6 mice/experimental group for all other ex vivo parameters (working heart perfusions).